

Real-time crash risk forecasting using Artificial-Intelligence based video analytics: A unified framework of generalised extreme value theory and autoregressive integrated moving average model

Fizza Hussain, Yasir Ali, Yuefeng Li, Md Mazharul Haque

PII: S2213-6657(23)00037-4

DOI: <https://doi.org/10.1016/j.amar.2023.100302>

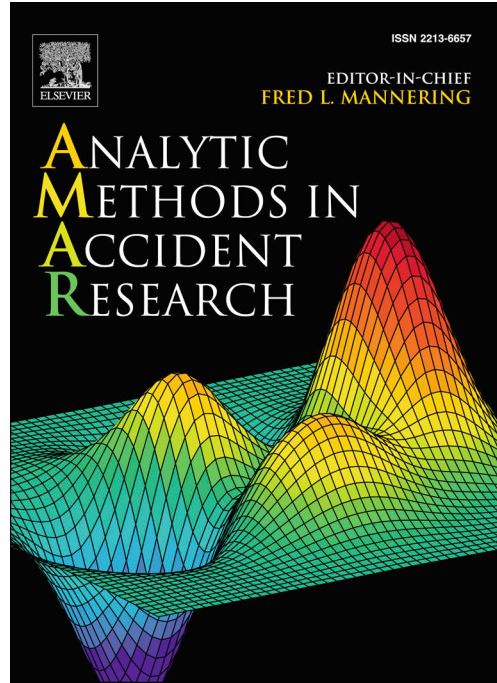
Reference: AMAR 100302

To appear in: *Analytic Methods in Accident Research*

Received Date: 4 May 2023

Revised Date: 3 September 2023

Accepted Date: 5 September 2023



Please cite this article as: F. Hussain, Y. Ali, Y. Li, M. Mazharul Haque, Real-time crash risk forecasting using Artificial-Intelligence based video analytics: A unified framework of generalised extreme value theory and autoregressive integrated moving average model, *Analytic Methods in Accident Research* (2023), doi: <https://doi.org/10.1016/j.amar.2023.100302>

This is a PDF file of an article that has undergone enhancements after acceptance, such as the addition of a cover page and metadata, and formatting for readability, but it is not yet the definitive version of record. This version will undergo additional copyediting, typesetting and review before it is published in its final form, but we are providing this version to give early visibility of the article. Please note that, during the production process, errors may be discovered which could affect the content, and all legal disclaimers that apply to the journal pertain.

Real-time crash risk forecasting using Artificial-Intelligence based video analytics: A unified framework of generalised extreme value theory and autoregressive integrated moving average model

Fizza Hussain

PhD candidate,

Queensland University of Technology,

School of Civil & Environment Engineering,

Faculty of Engineering,

Brisbane 4001, Australia.

Email: fizza.hussain@hdr.qut.edu.au

Yasir Ali

Lecturer,

School of Architecture, Building, Civil Engineering,

Loughborough University,

Leicestershire, LE11 3TU, United Kingdom.

Email: y.y.ali@lboro.ac.uk

Yuefeng Li

Professor,

Queensland University of Technology,

School of Computer Science,

Faculty of Science,

Brisbane 4001, Australia.

Email: y2.li@qut.edu.au

Md Mazharul Haque

(Corresponding author)

Professor,

Queensland University of Technology,

School of Civil and Environmental Engineering,

Faculty of Engineering,

Brisbane 4001, Australia

Email: m1.haque@qut.edu.au

ORCID ID: 0000-0003-1016-110X

August 2023

Abstract

With the recent advancements in computer vision and artificial intelligence, traffic conflicts occurring at an intersection and associated traffic characteristics can be obtained at the granular level of a signal cycle in real-time. This capability enables the estimation of the real-time crash risk using sophisticated modelling techniques, e.g., extreme value theory. However, these models are inherently incapable of forecasting the crash risk of future time periods based on the temporal dependency of crash risks. This study proposes a unified framework of extreme value theory and autoregressive integrated moving average models for forecasting crash risks at signalised intersections. At the first level of this framework, a non-stationary generalised extreme value model has been developed to estimate the real-time rear-end crash risk at the signal cycle level using the video data collected from three signalised intersections in Queensland, Australia. To capture the time-varying effect of different traffic conditions on conflict extremes, traffic flow, speed, shockwave area, and platoon ratio covariates are incorporated into the generalised extreme value model. The signal cycle-level crash risks obtained from the first level form a univariate time series, which is modelled using two variants of autoregressive integrated moving average model to forecast the crash risk of future signal cycles. Results reveal that the autoregressive integrated moving average model with exogenous variables outperforms the model without exogenous variables and can forecast the crash risk for the next 30–35 minutes with reasonable accuracy. Similarly, results also demonstrate that different crash risk patterns within a typical day are accurately predicted. The proposed framework helps identify the spatiotemporal windows where safety gradually deteriorates over time, thus enabling proactive safety assessment.

Keywords: Real-time; crash risk; forecasting; time-series models; signalised intersections.

1. Introduction

One of the fundamentals of proactive safety management is to assess and predict crash risk in real-time, which underpins devising mitigating strategies to prevent risk propagation and alleviate congestion. In general, real-time crash risk prediction aims to evaluate the riskiness of the existing traffic conditions within a short time window. Whilst assessing, it is hypothesised that the likelihood of a crash occurring in a particular time interval on a given road facility is a function of instantaneous prevailing traffic conditions. With such hypothesis, several studies were conducted for crash prediction, e.g., for rear-end crashes along motorways/freeways (Lee et al., 2003, Wang et al., 2019), city corridors (Chen et al., 2018), and signalised intersections (Zheng and Sayed, 2020, Fu and Sayed, 2022a, Ali et al., 2023b).

Although these studies serve as the steppingstones to realise the overarching concept of real-time safety, some drawbacks of earlier studies are summarised as follows. First, these studies frame crash risk prediction as a classification problem providing a binary outcome (crash or no crash), implying that it can only differentiate whether a crash will occur or not in given traffic conditions, whereas quantifying risky and crash-prone traffic conditions remains largely unexplored (Roshandel et al., 2015). Second, data obtained from loop detectors have limited behavioural information, and as such, understanding crash risk mechanisms and, consequently, predicting it with reasonable accuracy is nearly impossible. Third, most previous studies were focussed on real-time crash prediction on motorways/freeways, mainly because of the ease of obtaining loop detector data, as these road facilities are commonly equipped with various types of sensors. In contrast, signalised intersections have received relatively less attention for real-time crash risk prediction despite being a riskier road facility due to relatively higher traffic volume, and exhibiting stop-and-go movement (Yuan and Abdel-Aty, 2018, Ali

et al., 2021). Finally, these studies are not capable of forecasting crash risk for future time periods.

Previous studies primarily used police-reported crash data, which possess several limitations, such as under-reporting, low sample means, limited behavioural information, and omitted variable bias (Zheng et al., 2021). To overcome these issues, traffic conflicts can be used as they act as a precursor to crashes (Tarko, 2012) and eliminate the need for slowly accruing crash records for safety assessment. Traffic conflict techniques also facilitate proactive safety management as conflicts indicate an event in which a crash could happen but did not happen due to evasive action. To this end, a recent review paper (Ali et al., 2023a) highlights the research needs for linking conflicts with crashes using extreme value theory, and this study contributes along this direction.

Extreme value models have recently been developed to link conflicts with crashes and estimate the real-time crash risk (Zheng and Sayed, 2020, Ali et al., 2022a). Several studies have applied extreme value models for estimating crash risk at intersections (Songchitruksa and Tarko, 2006), motorways/freeways (Zheng et al., 2014, Ali et al., 2022b), and rural roads (Farah and Azevedo, 2017). Signalised intersections are of interest in this study as they are crash-prone locations because of frequent stop-and-go movements and drivers' tendency to follow too closely to pass through a green signal phasing, leading to high rear-end crash risk. A few studies have applied extreme value theory models to estimate real-time crash risk at signalised intersections (Zheng and Sayed, 2020, Fu and Sayed, 2022b, Ali et al., 2023b). These studies estimate signal cycle level crash risk as a step towards real-time safety analysis by estimating the crash risk of shorter time windows, as shown in Figure 1 (see purple box). It can be inferred from these studies that their focus remained on quantifying the crash risk of past time intervals. In contrast, the prime objective of real-time safety analysis is not only to understand/quantify the crash risk of time intervals that have passed but also to have the capability to estimate the crash risk for future time intervals (see the blue box in Figure 1) based on past and prevailing traffic conditions. This inability to predict crash risk in advance mainly stems from the use of extreme value theory models, which do not have the capability to forecast future crash risk based on the crash risk pattern that forms over time. This research gap motivates the present study.

In traffic safety literature, spatiotemporal correlation among crashes at a given site has been used to identify the safety deterioration that occurs over time (Chung et al., 2011) or to predict the short-term crash count (Bao et al., 2019). However, leveraging the temporal correlation among contiguous time intervals to predict the crash risk of future time intervals needs to be investigated carefully. For this purpose, using an appropriate time series model becomes paramount, and one such class of models is autoregressive integrated moving average. Whilst this model has been extensively used for traffic safety analysis (Noland et al., 2006, Quddus, 2008), its application for real-time safety analysis is scant, perhaps due to the unavailability of temporal crash risk data. With extreme value models being capable of providing crash risks at short time intervals utilising traffic conflicts, there is a great need to develop a joint modelling framework to forecast future crash risks.

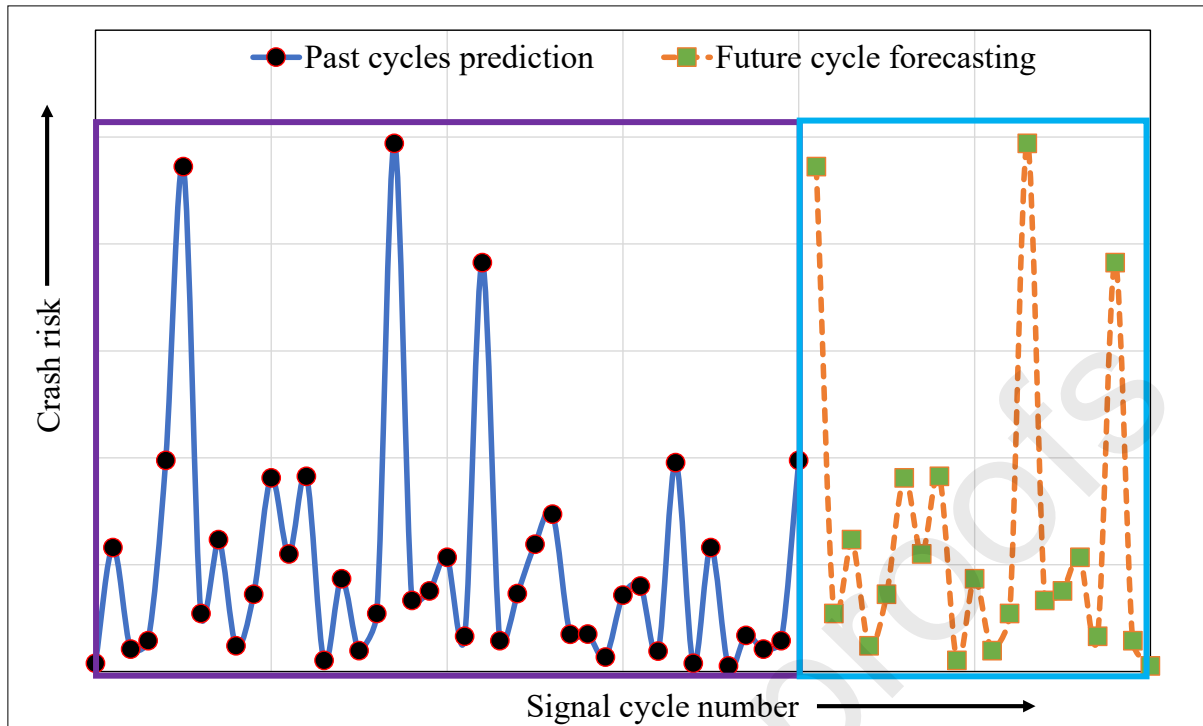


Fig. 1. A typical illustration of real-time crash risk estimation for signalised intersections

Table 1 summarises the representative studies on real-time safety analysis, and some key observations are as follows. First, two types of data sources are commonly used for real-time safety analysis (a) crash data coupled with loop detector data and (b) conflict data obtained from video recordings. For instance, Yu and Abdel-Aty (2013) used crash data and real-time traffic characteristics obtained from radar to develop support vector machine and Bayesian logistic regression models. These models were compared for crash occurrence prediction, and the support vector machine model performed better. Second, most of the methods used for analysis, which include logistic regression, artificial neural network, and long short-term memory network, require crash data and predict crash occurrence as a binary outcome. In contrast, extreme value theory models do not need crash data; instead, traffic conflicts are used to estimate crash risks (see a detailed discussion on traffic conflict measures in (Arun et al., 2021b, Arun et al., 2021c)). Extreme value models have the capability to provide (continuous values of) crash risk for short time windows, e.g., a signal cycle. Finally, despite several studies on real-time safety analysis, multi-step crash risk forecasting for future time periods has not been studied well. Although time series modelling techniques have the capability to forecast, their application for predicting crash risk of future time intervals has not yet been explored, which can be attributed to the limited availability of historical data on crash risk at the level of short time windows. These research gaps motivate the present study.

In traffic safety literature, some studies have adopted time series modelling, which enables predictions based on the forecasted variable's historical values. For example, Cai and Di (2023) have compared different forecasting methods for near future short-term crash prediction, including autoregressive integrated moving average model and some machine learning techniques, such as support vector machine, random forest, extreme gradient boosting, and negative binomial models. This study has used time series count data with traffic variables such as lane traffic flow, weather information, vehicle speed, and truck-to-car ratio to develop crash prediction models. Results revealed that the time series-based negative binomial model outperformed machine learning models for count data. Recently, a study developed an

autoregressive integrated moving average model to forecast annual crash fatalities for Australia using gender information, causes of crash deaths, and type of road users (Hassouna and Pringle, 2019). The model showed that male fatality rates were significantly higher than females, which was consistent with other countries. With an autoregressive integrated moving average model demonstrating reasonable forecasting capability for estimating crash risk with crash count data time series, an important research question is whether time series models are capable of forecasting crash risks estimated from traffic conflicts, which is explored in this study.

Table 1. Summary of representative real-time safety analysis studies

Study	Data	Crash risk calculation method	Crash risk forecasting
Yu and Abdel-Aty (2013)	Crash data and real-time traffic data detected by radars	Support vector machine and Bayesian logistic regression	×
Xu et al. (2013)	Crash data and loop detector data	Sequential logit model	×
Machiani and Abbas (2016)	Conflict data from radars	Safety surrogate histogram	×
Mussone et al. (2017)	Crash database and weather data	Back propagation neural network model and a generalised linear mixed model	×
Yuan and Abdel-Aty (2018)	(1) crash data (2) travel speed data collected by Bluetooth detectors; (3) signal phasing and 15 min interval traffic volume; (4) weather characteristics	Bayesian conditional logistic models	×
Yasmin et al. (2018)	(1) crash data, (2) weather data, (3) road geometry data, (4) traffic data collected from Microwave Vehicle Detection System (MVDS)	Multinomial logit model	×
Yuan et al. (2019)	(1) crash data, (2) travel speed data collected Bluetooth, (3) signal timing data, (4) loop detector data, and (5) weather characteristics	Long short-term memory network	×
Li et al. (2020)	(1) crash data, (2) signal timing, queue length, waiting time, and traffic volume, vehicle speed data collected through Bluetooth detectors, (3) and weather data	Long short-term memory convolutional neural network	×

Zheng and Sayed (2020)	Traffic conflicts from video data	Bayesian univariate extreme value model	×
Basso et al. (2021)	(1) crash data, (2) automated vehicle identification, (3) speed	Deep convolutional generative adversarial networks	×
Fu and Sayed (2022a)	Traffic conflicts from video data	Bayesian dynamic extreme value model	×
Fu and Sayed (2022b)	Traffic conflicts from video data	Bayesian bivariate extreme value model	×
Zhang and Abdel-Aty (2022)	(1) traffic flow data from loop detectors, (2) driver event variables from connected vehicle data	Bidirectional Long short-term memory network	×
Ding et al. (2022)	Crash data and traffic flow data	Negative Binomial model	×
Ali et al. (2023b)	Traffic Conflicts from video data	Bayesian univariate extreme value model	×

Note: highlighted rows indicate that these studies calculated crash occurrence as “yes” and “no” rather than quantifying the crash risk; ✓ and × respectively denote the presence and absence of that particular characteristic from a study.

This study proposes a unified framework of extreme value theory and autoregressive integrated moving average model to forecast crash risk at signalised intersections. The developed framework is tested using traffic conflicts obtained from video data collected in Brisbane, Queensland, Australia.

The contribution of this study is threefold. First, the proposed framework brings together the capabilities of extreme value theory and autoregressive integrated moving average models to complement each other. More specifically, an extreme value theory model can provide serially correlated continuous crash risk values for short time windows (e.g., signal cycles) but does not have the capability to forecast crash risk for future time periods. In contrast, an autoregressive integrated moving average model can forecast crash risk based on temporally correlated data, which can be obtained from extreme value models. Second, this study thoroughly compares the performance of different variants of autoregressive integrated moving average models for real-time crash risk forecasting, which will provide justification for adopting a particular model for real-time crash risk analysis. Finally, the proposed framework will facilitate proactive safety assessment by providing crash risks of future time intervals. The proposed framework will be helpful for road traffic authorities in determining risky time intervals well in advance so as to devise effective crash mitigation strategies.

The rest of the paper is structured as follows. Section 2 explains the study methodology, including model development, whereas Section 3 describes data collection and its pre-processing. Whilst Section 4 summarises the study results, which are discussed in Section 5. Finally, Section 6 concludes the study and pinpoints future research directions.

2. Methodology

This study presents a unified crash risk forecasting framework for signalised intersections, as illustrated in Figure 2. Video recordings of vehicle movements at signalised intersections were collected from three intersections (more details in the next section). Artificial intelligence-based automated video analytics were employed to process the videos to generate vehicle trajectories and conflicts through Advanced Mobility Analytics Group's SMART Safety™ platform (AMAG, 2021). Trajectories, conflicts, and loop detector data were fused together to compute signal cycle level covariates using an automated covariate extraction algorithm (Ali et al., 2023b). These covariates are incorporated into the extreme value model to handle the non-stationary traffic conflict extremes and explain the crash risk. The performance of the developed extreme value model is evaluated at a macro level to estimate annual crash counts and then applied to estimate signal cycle level crash risk. These continuous values of signal cycle level crash risk form a time series, which are fed to an autoregressive integrated moving average model for crash risk forecasting. Ensuing subsections describe the development of extreme value theory and autoregressive integrated moving average models in detail.

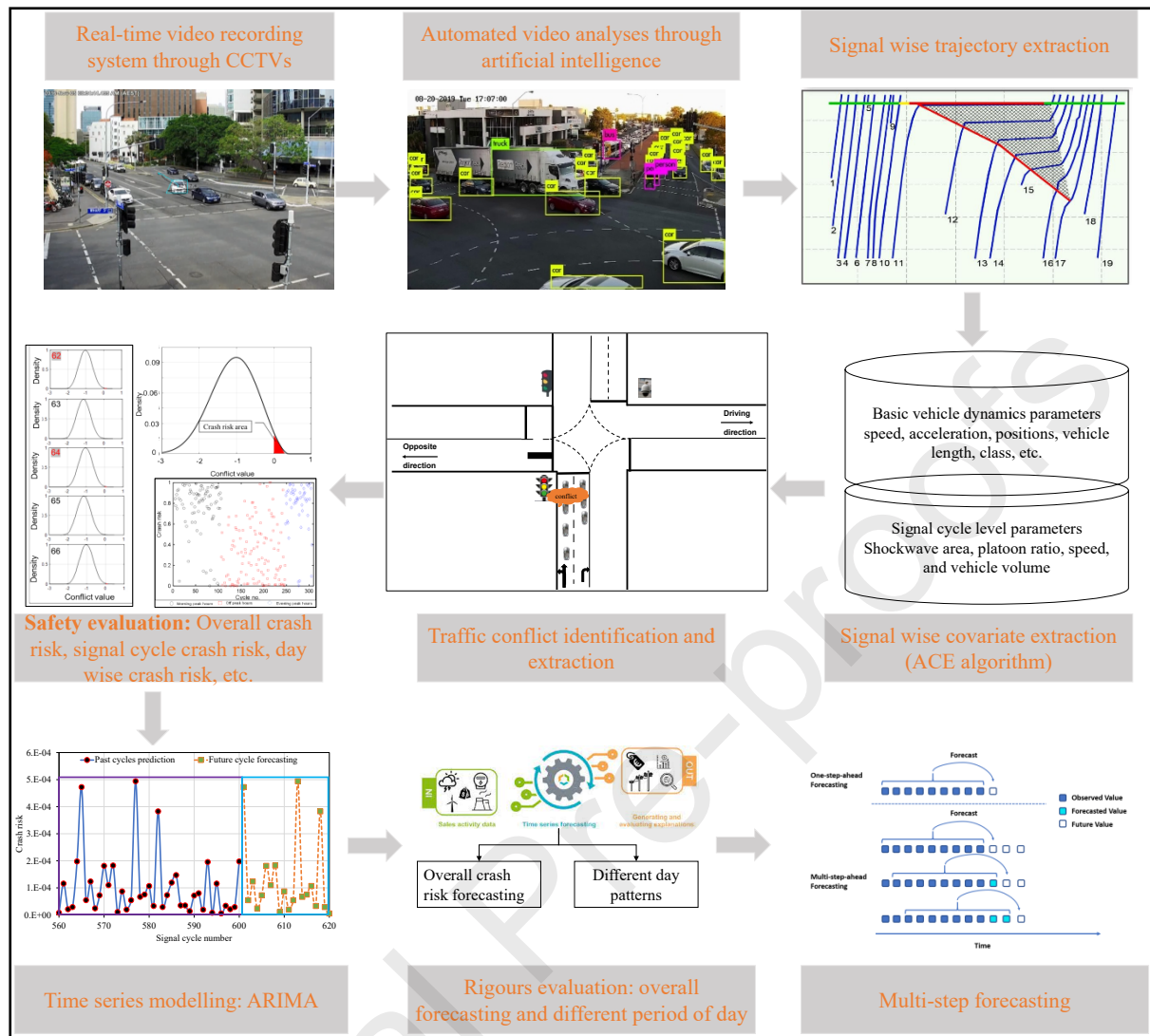


Fig. 2. Unified real-time crash risk forecasting framework

2.1 Extreme value model

An extreme value theory approach is adopted to estimate the crash risk at the signal cycle level. This approach can extrapolate crash risk from frequently observed events (i.e., traffic conflicts) to rare events (i.e., crashes). Due to this unique feature, the extreme value theory approach eliminates the need for crash data for model estimation and instead uses traffic conflicts as crash precursors. To this end, the block maxima approach, corresponding to a generalised extreme value distribution, is applied. As the block maxima approach is based on the time domain, traffic conflict extremes must be sampled in a continuous time domain. This study selects the signal cycle as the time window, as signal cycles serve as the natural block for a signalised intersection. Assume that $z_1, z_2, z_3, \dots, z_n$ be a sequence of random and independent variables with a common distribution function and $M_n = \max(z_1, z_2, z_3, \dots, z_n)$ yields the maximum of n values in a block. In the proposed framework, z_i refers to a traffic conflict measure during signal cycle i . Note that the proposed block maxima model can be applied to any conflict measure; however, care must be exercised whilst sampling extremes as minima/maxima are dependent on the type of conflict measure. With a sufficiently large sample

size, it is assumed that $M_n = \max(z_1, z_2, \dots, z_n)$ will converge to a generalised extreme value distribution when $n \rightarrow \infty$, which can be mathematically defined as

$$G(z) = \exp\left(-\left[1 + \xi\left(\frac{z - \mu}{\sigma}\right)\right]^{-1/\xi}\right), \quad (1)$$

where $-\infty < \mu < \infty$ refers to the location parameter, $\sigma > 0$ represents the scale parameter, and $-\infty < \xi < \infty$ denotes the shape parameter. From the fitted generalised extreme value distribution, crash risk can be calculated as

$$RC_i = Pr(z_i \geq 0) = 1 - G_i(0) = \begin{cases} 1 - \exp\left(-\left[1 - \xi_i^{\mu_i}\right]^{-\frac{1}{\xi_i}}\right), & \text{for } \xi \neq 0 \\ 1 - \exp\left[-\exp\left(\frac{\mu_i}{\sigma_i}\right)\right], & \text{for } \xi = 0 \end{cases} \quad (2)$$

where, RC_i represents the risk of a crash in a signal cycle i , and $G(\cdot)$ is the fitted generalised extreme value distribution. The risk of a crash is nonnegative, with a value of zero indicating no crash risk for a given cycle (or a safe cycle) and a value greater than zero indicating a positive crash risk in a given signal cycle. Note that Eq. (2) is applicable to temporal proximity measures, whereas for other measures like spatial or kinematic, it needs modification.

This study applies the proposed framework (and the block maxima model, as shown in Eq. (1)) to model rear-end conflict extremes. Ensuring the scale parameter to be positive, this study parameterises scale parameter as $GEV(\mu, \phi, \xi)$, where $\phi = \log \sigma$ and GEV refers to generalised extreme value. Let z_{ij} be the maximum value of a traffic conflict measure for the i^{th} cycle for a site j , with $j = 1, 2, \dots, s$, and $i = 1, 2, \dots, n_j$, a site-wise generalised extreme value distribution, can be obtained as

$$G(z_{ij} < z | \mu_{ij}, \phi_{ij}, \xi_{ij}) = \exp\left(-\left[1 + \xi_{ij}\left(\frac{z - \mu_{ij}}{\exp(\phi_{ij})}\right)\right]^{-1/\xi_{ij}}\right). \quad (3)$$

Time-varying factors, such as traffic conditions, may affect rear-end conflicts. As such, estimating the generalised extreme value model without incorporating these factors may lead to time-varying unobserved heterogeneity, which may affect model performance (Songchitruksa and Tarko, 2006). To address this issue, several covariates have been included in the generalised extreme value model parameters (except for the shape parameter that is difficult to estimate precisely, as noted by Coles (2001)). An identity link function has been adopted to incorporate covariates in the generalised extreme value model. Mathematically, generalised extreme value distribution parameters can be re-parameterised as

$$\begin{cases} \mu_{ij} = \alpha_{\mu 0} + \alpha_{\mu 1} \mathbf{X} + \varepsilon_{\mu j} \\ \phi_{ij} = \alpha_{\phi 0} + \alpha_{\phi 1} \mathbf{Y} + \varepsilon_{\phi j} \\ \xi_{ij} = \alpha_{\xi 0} + \varepsilon_{\xi j} \end{cases}, \quad (4)$$

where, $\alpha_{\mu 0}$, $\alpha_{\phi 0}$, and $\alpha_{\xi 0}$ are intercept terms for each model parameter, $\alpha_{\mu 1}$ and $\alpha_{\phi 1}$ are parameter estimates for the covariate vectors \mathbf{X} and \mathbf{Y} , respectively, and $\varepsilon_{\mu j}$, $\varepsilon_{\phi j}$, and $\varepsilon_{\xi j}$ are random error terms. Random error terms in Eq. (4) represent between-site variances, which remain constant for traffic conflict extremes at a site but vary among different sites. As such,

the same process described in Equation (4) can also be expressed as a random intercept model as

$$\begin{cases} \mu_{ij} = \alpha_{\mu j} + \alpha_{\mu} X \\ \phi_{ij} = \alpha_{\phi j} + \alpha_{\phi} Y \\ \xi_{ij} = \alpha_{\xi j} \end{cases}, \quad (5)$$

The Bayesian estimation process is applied for estimating the parameters of generalised extreme value theory model, which is suitable for obtaining posterior distributions and specifying priors for model parameters to characterise the latent process. Uninformative priors are assigned for all model parameters due to a lack of information on how generalised extreme value parameters vary. Priors are assumed to follow a normal distribution with mean zero and large variance, $N(0, 10^6)$. The literature has reported that improper priors assigned to the shape parameter can potentially lead to model convergence issues (Zheng and Sayed, 2020, Zheng et al., 2021). To address this issue, prior information from some previous studies (Songchitruksa and Tarko, 2006, Zheng et al., 2014, Zheng et al., 2019, Zheng and Sayed, 2019) is used to select the value of the shape parameter between the range of $(-1.0, 1.0)$. As such, the prior for the shape parameter is defined as $\alpha_{\xi j} \sim \text{unif}(-1.0, 1.0)$.

For the Bayesian generalised extreme value model presented in Eq. (5), likelihood functions are built from probability distributions obtained from Eq. (3), and prior distributions are assigned to parameters in Eq. (5). In other words, the posterior probabilities of model parameters are a function of probabilities assigned in Eq. (3). This study obtains the posterior distributions of model parameters using Markov Chain Monte Carlo simulation, where Gibbs sampling is used.

Several Bayesian generalised extreme value models are developed using different combinations of covariates. Deviance Information Criterion (DIC) is used to compare the performance of competing models (Spiegelhalter et al., 2002), which can be computed as

$$DIC = \bar{D} + p_D, \quad (6)$$

where \bar{D} is the posterior mean deviance that measures the model fitting and p_D is the effective number of parameters in the model. In general, a smaller value of the deviance information criterion indicates a better model fit. The best model is selected from the suite of developed models using the smallest deviance information criterion value.

2.2 Autoregressive integrated moving average model

For modelling univariate time series data, Box and Jenkins (1976) combined autoregressive models and moving average models to develop an autoregressive integrated moving average (ARIMA) model that explicitly includes differencing, which is suitable for time series analysis. The autoregressive component of ARIMA captures the time series nature of data by relating the current observation with its previous observations, whereas the moving average component explains time series as a linear function of current and preceding random errors. Mathematically, an ARIMA model can be expressed as

$$\nabla^d y_t = \frac{\theta(B)}{\varphi(B)} \epsilon_t, \quad (7)$$

where, y_t denotes the response time series variable (i.e., crash risk for time interval t), ϵ_t is a random error term, B represents a backshift operator, ∇ indicates the integrated processes ($\nabla y_t = y_t - y_{t-1}$), and d represents the order of non-seasonal differences required to achieve time series stationarity. Further, $\theta(B)$ and $\varphi(B)$ can be obtained as

$$\theta(B) = (1 - \theta_1B - \theta_2B^2 - \dots - \theta_qB^q), \quad (8)$$

$$\varphi(B) = (1 - \varphi_1B - \varphi_2B^2 - \dots - \varphi_pB^p), \quad (9)$$

where, $\theta_1, \theta_2, \dots, \theta_q$ are moving average parameters and $\varphi_1, \varphi_2, \dots, \varphi_p$ are the autoregressive parameters. An autoregressive integrated moving average (ARIMA) model is expressed as ARIMA (p, d, q) , whereby p , d , and q respectively refer to the order of autoregressive, non-seasonal difference, and moving average parts.

The autoregressive integrated moving average model with exogenous variables (ARIMAX model) is an extension of the standard ARIMA model, which incorporates of the effects of exogenous variables on time series. The ARIMAX model adopted in this study is a multiple-input, single-output transfer function model, as shown in Equation (10), which is a straightforward extension of Equation (7) as

$$y_t = \sum_{i=1}^p \varphi_i y_{t-i} + \sum_{k=1}^r \beta_k X_{tk} + \epsilon_t + \sum_{j=1}^q \theta_j \epsilon_{t-j}, \quad (10)$$

where, vector X denotes the values of the r exogenous, time-varying predictors at time t, with coefficients denoted β . Note all other variables are explained previously.

Statistically significant autoregressive integrated moving average models are developed to forecast crash risks following a three-step iterative process for selecting the parsimonious models. The details of each step are provided in the ensuing subsections. Note that these steps are applied to both ARIMA and ARIMAX models.

2.2.1 Model identification

The first step in developing an autoregressive integrated moving average model is to identify whether the time series is stationary. A stationary time series does not have any trend or seasonal component, and its statistical properties (e.g., mean, variance, covariance, etc.) do not vary with time. Autocorrelation function plots and the Augmented Dickey-Fuller test are used to confirm or reject the presence of stationarity in the time series of crash risk data. Mathematically, the Augmented Dickey-Fuller regression equation can be obtained as (Dickey and Fuller, 1979)

$$y_t = \alpha + \rho y_{t-1} + \sum_{i=1}^k \varphi_i \Delta y_{t-i} + \beta t + \varepsilon_t, \quad (11)$$

where, Δy_{t-i} denotes the time-lagged change in the response variable (i.e., crash risk). Note that all other variables in Equation (10) are described previously. The null hypothesis in this test is that there exists non-stationarity in time series, i.e., it does not have a constant mean and variance over time. If the time series is non-stationary, it is treated with differencing to obtain stationarity, which is a prerequisite for determining the autoregressive and moving average components using the autocorrelation function and partial autocorrelation function.

2.2.2 Model parameter estimation

Model parameters are estimated using a maximum likelihood method, and conventional procedures (e.g., *t*-statistics and confidence interval) are used to assess the significance of model parameters. Since several models are estimated with and without exogenous variables, the parsimonious model is selected based on the lowest Bayesian Information Criterion (BIC) value.

2.2.3 Model diagnostic checking

Autocorrelation and partial autocorrelation plots of the residuals are used to assess the adequacy of the developed model. Ljung-Box statistic (Q^*) is calculated as (Ljung and Box, 1978)

$$Q^* = n(n + 2) \sum_{j=1}^p \frac{r_j^2}{n-j}, \quad (12)$$

where, r_j , n , and p indicate residual autocorrelation parameters at lag j , number of residuals, and number of time lags in the test, respectively. If the resulting *p*-value of Q^* statistic is smaller than the assumed significance level, the model deems unsatisfactory and requires modifications.

3. Datasets used for analysis

3.1 Video data collection and processing

Video data were collected from three signalised intersections in South-East Queensland, Australia, as shown in Figure 3. These intersections are similar in their geometric layout and operations and fall within the same jurisdiction. Dedicated overhead cameras were installed on 6.5 m high poles for video data collection at each intersection, whereby cameras covered the intersection areas shown in triangles and 30 m along each approach, as shown in Figure 3. For each intersection, 12 hours (from 6 am to 6 pm) of video data were collected for four days (Tuesday to Friday).



(a) Granard Rd – Beaudesert Rd Intersection



(b) Logan Rd – Kessels Rd Intersection



(c) Appleby Rd – Stafford Rd Intersection

Fig. 3. Camera positions and their coverages.

An automated video analysis platform was used to process video footage. Key steps in video data processing include camera calibration, object detection, tracking, trajectory extraction, and conflict identification (see Figure 4 for an illustration). Whilst a detailed description of video processing is omitted from this paper to avoid overlap with other studies, interested readers are referred to our earlier studies (Hussain et al., 2022, Arun et al., 2021a). Succinctly, the YOLO algorithm was used for object detection, and the DeepSORT algorithm tracked the movement of the detected objects or road users. Using a trajectory overlapping technique, rear-end traffic conflicts were identified and measured by modified time-to-collision (see Eq. 12) (Ozbay et al., 2008). A 3-second threshold was used for identifying traffic conflicts using the time-to-collision and called traffic conflicts. This study adopts the modified time-to-collision (MTTC) measure to model rear-end crash risk. Note that whilst the threshold is placed on time-to-collision, it may not necessarily mean that the modified time-to-collision value would be less than 3 s, as reflected in Table 2.

$$MTTC_t = \frac{\Delta v_t \pm \sqrt{\Delta v_t^2 + 2\Delta a_t(x_{L,t} - x_{F,t} - D_L)}}{\Delta a_t}, \quad (13)$$

where MTTC refers to modified time-to-collision, $\Delta v_t = v_{F,t} - v_{L,t}$ is the relative speed of the conflicting vehicles at time t , $x_{L,t}$ and $x_{F,t}$ are the positions of the leading vehicle and the

following vehicle at time t , respectively; $\Delta a_t = a_{F,t} - a_{L,t}$ is the relative acceleration of the conflicting vehicles at time t ; D_L is the length of the leading vehicle.

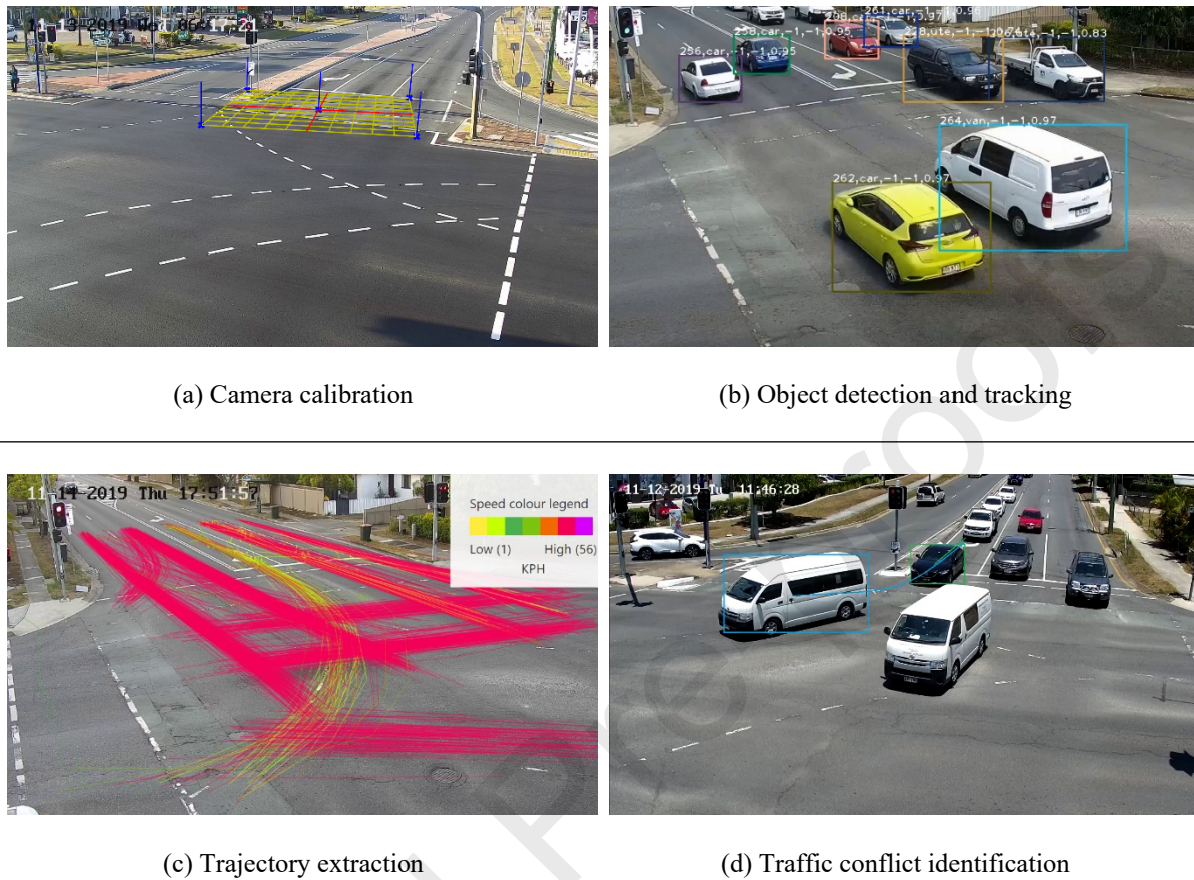


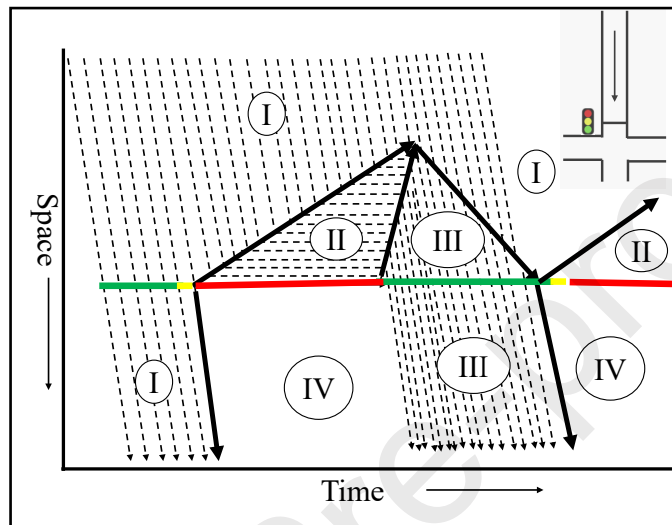
Fig. 4. Traffic conflict identification process using artificial intelligence techniques

3.2 Extracting covariates for the extreme value theory model

Obtaining signal cycle level covariates that can account for non-stationarity of conflict extremes is non-trivial due to multiple data sources being involved in this process. These data sources are trajectories, traffic conflicts extracted from the automated video analysis platform, and loop detector data (containing information on signal timing and phasing) obtained from road authorities. To process these datasets simultaneously and obtain required signal cycle level covariates, this study adapts the automated covariate extraction algorithm (Ali et al., 2023b) for rear-end conflicts. This algorithm is designed on the data fusion principles of Dasarathy's classification, that is, data in-feature out (Castanedo, 2013). Raw (or processed) data from different sources have been combined to extract relevant traffic characteristics at the signal cycle level.

The following steps are performed to obtain covariates from various data sources. First, timestamps of each signal cycle in the trajectory and conflict datasets are identified, which ensures matching the correct trajectory of the conflict to its corresponding cycle where it is recorded. Second, signal cycle numbers are assigned to each conflict acquired from the video analysis platform. Additionally, signal information such as green, yellow, and red phases are assigned to conflicts and trajectories. Therefore, loop detector data are not required for further

data processing steps. In the next step, signal cycles containing rear-end conflicts are identified and considered for further processing. Finally, from each signal cycle, covariates characterising the crash risk of each block (i.e., signal cycle) are computed. These covariates are traffic flow (number of vehicles per signal cycle on a given lane), shockwave area (the triangle area where the traffic flow state is II following the four traffic flow states theory (May, 1990), see Figure 5), platoon ratio (proportion of vehicles arriving during the green phase multiplied by the ratio of the signal cycle length to the effective green time of the subject movement (HCM, 2000)), and average speed of vehicles during the signal cycle. The descriptive statistics of these covariates are presented in Table 2.



Description: I, II, III, and IV denote free flow traffic state, standstill (or traffic jam), traffic flow at capacity (or steady-state flow), and no traffic flow, respectively.

Fig. 5. Space-time diagram for extracting signal cycle level covariates

3.3 Crash data

Crash records of the study sites for the years 2015-2019 were obtained from the Department of Transport and Main Roads, Queensland, for model validation. Filters were applied to the crash data to avoid any discrepancy between obtained traffic conflicts and crashes to match them with the conditions in which video data were captured. These filters selected only the rear-end crashes that occurred during weekdays (Tuesday – Friday), during the daytime (6 am – 6 pm), and during fair weather conditions. As such, a total of 31 crashes were observed for three intersections, with 16, 9, and 6 crashes corresponding to Beaudesert Rd – Granard Rd, Kessels Rd – Logan Rd, and Appleby Rd – Stafford Rd intersections, respectively.

Table 2. Descriptive statistics of traffic conflicts and traffic operational variables

Intersection	Indicator	Mean	SD	Minimum	Maximum
Appleby-Stafford	MTTC (s)	1.665	0.646	0.133	4.655
	Flow (veh/cycle)	7.577	2.449	1.000	18.000

	Speed (m/s)	3.535	1.237	1.218	9.414
	Shockwave area (km.s)	3.079	1.450	0.010	9.136
	Platoon ratio	2.149	0.630	0.092	4.842
	Number of cycles	632			
Beaudesert-Granard	MTTC (s)	1.553	0.622	0.711	4.510
	Flow (veh/cycle)	8.904	6.818	1.000	17.000
	Speed (m/s)	5.262	1.423	1.2028	10.157
	Shockwave area (km.s)	2.695	0.057	0	7.263
	Platoon ratio	2.199	1.105	0.054	5.141
	Number of cycles	531			
Logan-Kessel	MTTC (s)	1.66	0.638	0.361	5.046
	Flow (veh/cycle)	2.363	4.065	1.000	28.000
	Speed (m/s)	3.709	1.009	1.150	8.440
	Shockwave area (km.s)	2.965	1.462	0.027	7.556
	Platoon ratio	2.352	0.863	0.057	4.939
	Number of cycles	617			

Abbreviations: *SD: standard deviation; MTTC: modified time-to-collision*

4. Results

This study separately develops the generalised extreme value model and autoregressive integrated moving average (ARIMA) models. The former model is estimated in the Bayesian framework, whereas the latter model is estimated using a maximum likelihood approach.

4.1 Extreme value model

4.1.1 Model selection

The data from three intersections are combined to develop the extreme value model. To handle the non-stationarity of traffic extremes and incorporate time-varying crash risk, covariates are added to model parameters in three arrangements: (1) parameterising the location parameter, (2) parameterising the scale parameter, and (3) parameterising both the scale and location parameters. These models are also compared with a stationary model where no covariates were included. For each of the non-stationary models, different combinations of covariates are tested, and the best model was selected on the basis of goodness-of-fit measures.

These models are estimated in the Bayesian framework with two separate chains for each model parameter with different initial values. The total iterations were set as 50,000 from which the initial 20,000 iterations were considered burn-in samples and thus discarded. The rest of the iterations were used for obtaining posterior estimates. The convergence of all the models was checked by calculating the Gelman-Rubin statistics and trace plots. The value of Gelman-Rubin statistics was close to 1.1, indicating the model convergence. Similarly, the trace plots show that both chains are well mixed with each other, providing further evidence of model convergence.

The deviance information criterion is used for local goodness-of-fit to compare different model variants. The deviance information criterion (DIC) values are 14553, 14772, 15569, and 17889 for the model with parameterised location parameter, the model with parameterised scale parameter, the model with parameterised both location and scale parameters, and the stationary model, respectively. Compared to the stationary model, all non-stationary model variants resulted in lower deviance information criterion values, indicating their better goodness of fit. Among three non-stationary models, the model with parameterised location parameter resulted in the lowest deviance information criterion, suggesting the best-fit model for the dataset.

4.1.2 Model interpretation

Model estimation results are presented in Table 3. Four covariates are included in the location parameter: traffic flow within a signal cycle, the average speed of vehicles in a cycle, shockwave area and platoon ratio. Although the parsimonious model only contains four covariates, several other variables were tested in the model, such as signal cycle duration and the number of conflicts in a signal cycle. These variables were excluded from the final model because they (a) were found to be not significant (assessed by Bayesian credible intervals), (b) did not improve the model fit, and (c) neither improved mean crash estimates nor confidence intervals. All four statistically significant parameters possessed intuitive signs, as presented in Table 3.

Table 3. Generalised extreme value model estimation results

Parameter	Description	mean	Standard deviation	Bayesian credible interval	
				2.5%	97.5%
$\mu_{Appleby}$	Location intercept (Appleby)	1.080	0.093	0.883	2.649
$\mu_{Beaudesert}$	Location intercept (Beaudesert)	1.011	0.009	0.894	3.939
μ_{Logan}	Location intercept (Logan)	0.673	0.090	0.003	0.925
$\alpha_{\mu[Flow]}$	Traffic flow (veh/cycle) in a cycle	0.454	0.072	0.1472	0.488
$\alpha_{\mu[Speed]}$	Average speed (m/s) in a cycle	0.291	0.039	0.129	0.798
$\alpha_{\mu[Shockwave area]}$	Shockwave area (km.s)	0.246	0.092	0.084	0.665
$\alpha_{\mu[Platoon ratio]}$	Platoon ratio	-1.159	0.340	-5.915	-0.657
$\phi_{Appleby}$	Scale parameter (Appleby)	0.324	0.020	0.034	0.741
$\phi_{Beaudesert}$	Scale parameter (Beaudesert)	0.847	0.050	0.145	1.325
ϕ_{Logan}	Scale parameter (Logan)	0.0069	0.001	0.0005	0.001
$\xi_{Appleby}$	Shape parameter (Appleby)	-0.305	0.014	-0.538	-0.137
$\xi_{Beaudesert}$	Shape parameter (Beaudesert)	-0.047	0.014	-0.024	-0.015
ξ_{Logan}	Shape parameter (Logan)	-0.003	0.0004	-0.0028	-0.237

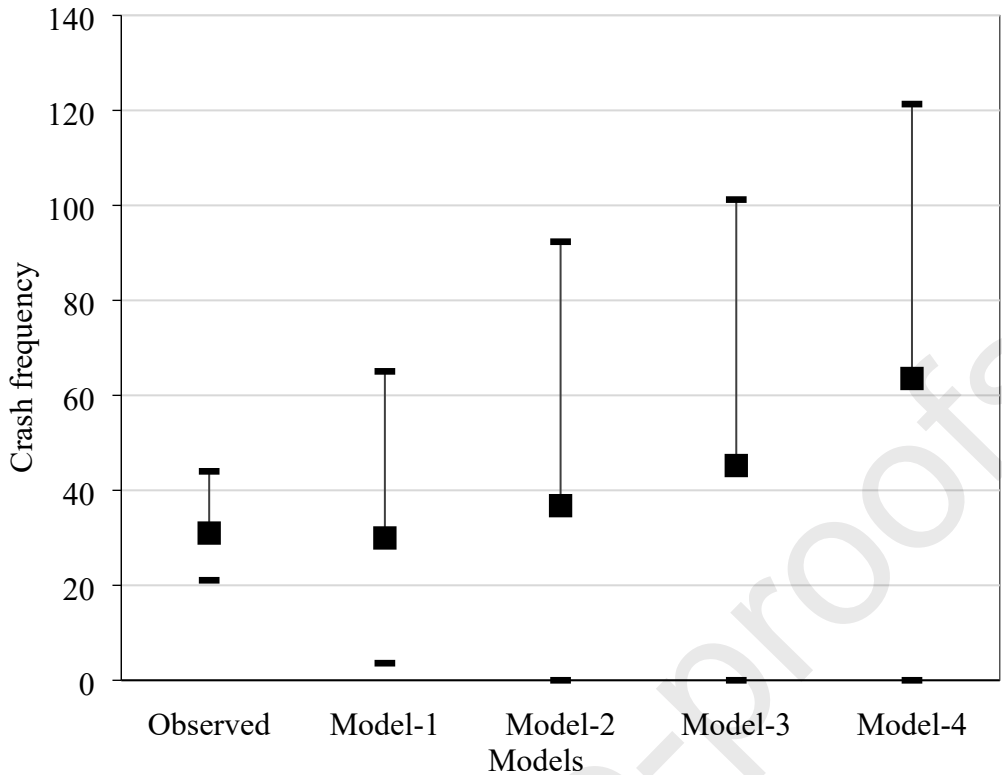
Model statistics: Deviance information criterion = 14553

Observed crashes for five years (confidence interval): 31 (21.06 – 44)

Estimated crashes for five years (confidence interval): 29.97 (0 – 95.05)

4.1.3 Model validation

The model presented in Table 3 is validated against historical crash records (i.e., observed crashes) that occurred at the study sites. Conventionally, the estimated crashes from the model fitted to signal cycle level data are compared with aggregated crashes. Ideally, model performance should be validated at the signal cycle level to confidently adopt the model for practical use. However, this validation may not be possible. Therefore, this study adopts the conventional approach to validate the model performance at the aggregate level. Both mean crash estimates and the corresponding confidence intervals are compared. Mean estimated crashes for n years can be calculated using the developed model as $N = \frac{\tilde{T}}{T}RC$, where N denotes the expected number of crashes that occurred during the duration \tilde{T} , T is the data collection duration, and RC is the risk of a crash. If $\tilde{T} = 5$ years, then N reflects the expected number of crashes for five years. The confidence intervals, characterising the uncertainty associated with model predictions, were obtained using a simulation method (Songchitruksa and Tarko, 2006). Using a predefined iteration of 30,000, the distributions of model parameters are obtained that can be used to calculate the 95th percentile of the distribution. For calculating the confidence interval of the observed crashes, the 95% Poisson confidence interval (Songchitruksa and Tarko, 2006) of the observed crashes using the true mean annual crashes, λ , is computed as $[\lambda - \frac{1}{2N}\chi^2_{2y_0, 0.975} \leq \lambda \leq \frac{1}{2N}\chi^2_{(2y_0 + 1), 0.025}]$, where $N = 5$ years, and y_0 indicates the total number of crashes in the 5-year period for the study site. The comparison of observed crashes and estimated crashes by the stationary and various non-stationary models is presented in Figure 5. It is evident from Figure 6 that the stationarity model, which shows the worst fit, also yields the widest confidence intervals. In contrast, the model with parameterised location parameter shows relatively better mean crash estimates and narrower confidence intervals. For instance, the mean crash estimate for this model is 29.97, which is very close to the mean observed crashes of 31. Similarly, the range of confidence interval is calculated (difference of upper and lower intervals), which is about 2.67 times more than the confidence intervals of observed crashes, whereas the ranges of confidence intervals for other models are much wider. These results confirm the adequacy of the developed model in estimating the observed crashes.



Description: Model-1: Model with parameterised location parameter; Model-2: Model with parameterised scale parameter; Model-3: Model with parameterised both location and scale parameters; Model-4: Stationary model.

Fig. 6. Comparison of different generalised extreme value theory model variants for estimating crashes

4.1.4 Model application: signal cycle level crash estimation

The developed model generates site-specific and signal cycle-wise generalised extreme value distributions. As an illustration, the distributions of six signal cycles (selected randomly) from each intersection are generated and shown in Figure 7. Note that the numbers inside each subfigure indicate the signal cycle number, and the signal cycle number in red indicates a signal cycle with positive crash risk. The shape of the distribution provides insights into traffic conditions that lead to the identification of risky or safe cycles. More specifically, the tail of a generalised extreme value distribution ending after the negated modified time-to-collision (MTTC) = 0 indicates a positive crash risk.

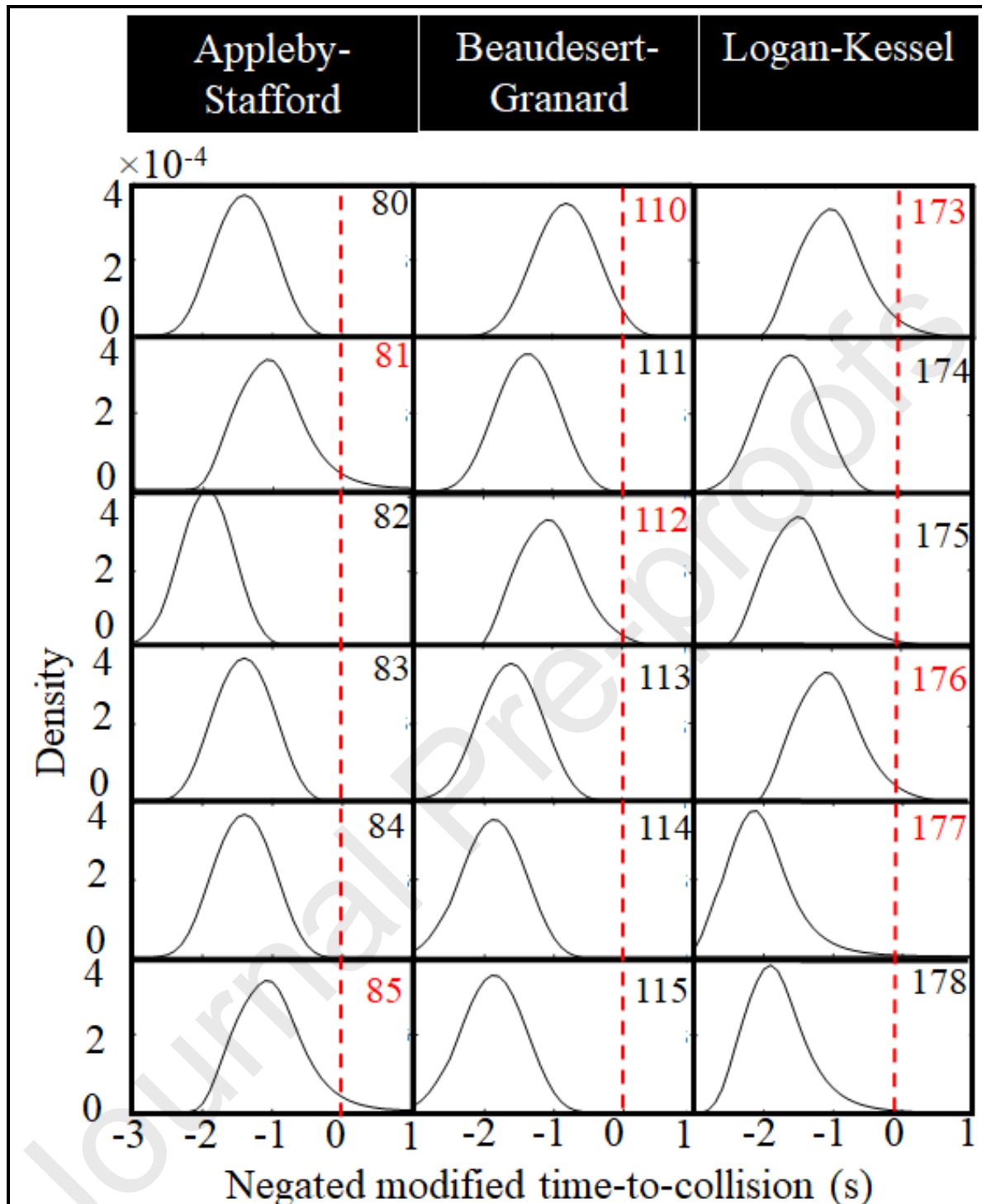


Fig. 7. Generalised extreme value distributions for some representative signal cycles

Figure 7 indicates that two (out of six) cycles (81 and 85) for the Appleby-Stafford Road intersection exhibit positive crash risk since their distributions cross the negated MTTC = 0 point. For the Granard-Beaudesert Road and Logan-Kessel Road intersections, two and three risky signal cycles are found as risky, respectively, as their distributions cross negated MTTC = 0 points.

From the fitted generalised extreme value distribution of each signal cycle, the crash risk of the corresponding signal cycle is obtained using Equation 2. The signal cycle level crash

risks are used to develop and test the performance of the autoregressive integrated moving average models, and the results are described in the next subsection.

4.2 Autoregressive integrated moving average model

4.2.1 Handling discontinuity in time series

It is quite common in real life that conflicts may not occur regularly or in every given time interval, e.g., each signal cycle, leading to no conflicts in some cycles. This issue leads to a discontinuous crash risk time series, which violates the assumption of conventional time series modelling, i.e., time series data should be continuous (or a continuous time series). To this end, this study applies a zero-padding approach whereby zero crash risk is assigned to signal cycles where no conflict occurs. Theoretically, it can be justified as no conflict in a given cycle reflects no (or negligible) crash risk, which can be denoted by zero value in the crash risk time series. By doing so, this study makes crash risks as continuous time series with equally spaced time intervals, making it suitable to be modelled by an autoregressive integrated moving average model.

4.2.2 Testing stationarity of crash risk time series

The time series plot of the crash risk of contiguous signal cycles, shown in Figure 8, indicates how crash risk varies over time. Note that this crash risk in Figure 8 is obtained from the Bayesian extreme value model (see Section 5.1 for more details) for one day of Appleby-Stafford Intersection, and similar figures for other intersections are not presented for brevity. It can be observed from Figure 8 that there is no trend or evident seasonality component, reflecting the stationary of the time series. In such a scenario, no transformation or differencing is required to stabilise the variance in the series. To further confirm the stationary of the time series, an Augmented Dickey–Fuller test is applied for all the time periods of all intersections. As an illustration for one day of Appleby-Stafford Intersection, the Dickey–Fuller test reveals that the crash risk data (or time series) is stationary (*test statistic* = 13.74; *p-value* < 0.001), which implies that our time series does not require any differentiation to make it stationary. Similar results are obtained for all time periods and other intersections.

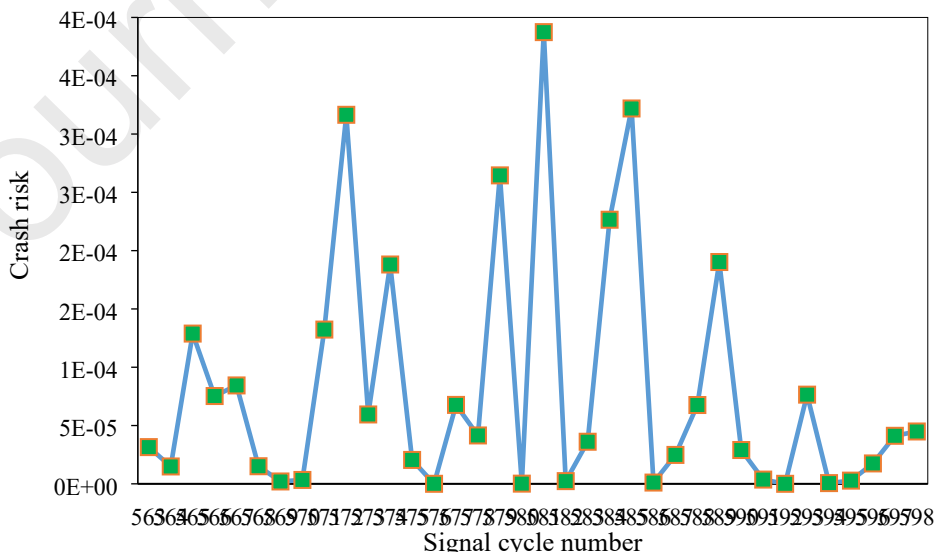


Fig. 8. Crash risks time series of one day for Appleby-Stafford Intersection

4.2.3 Model selection

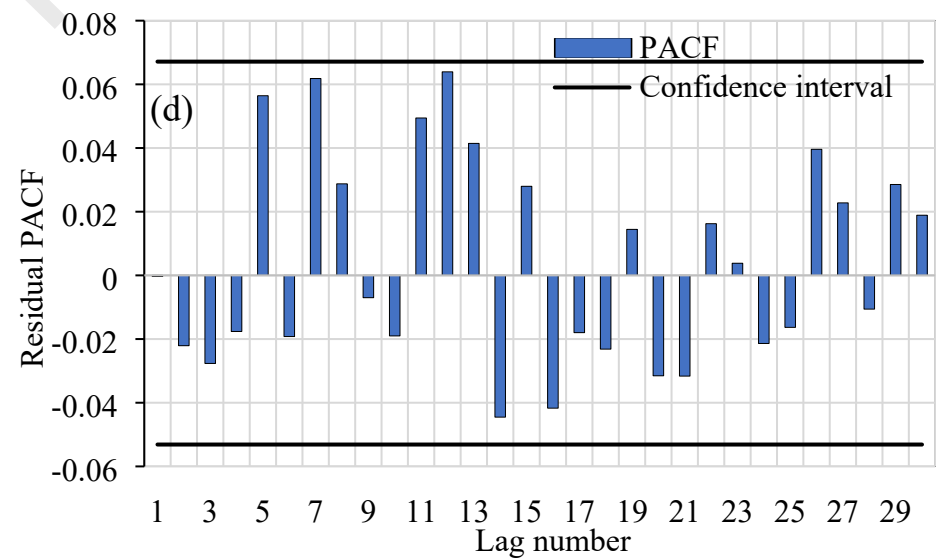
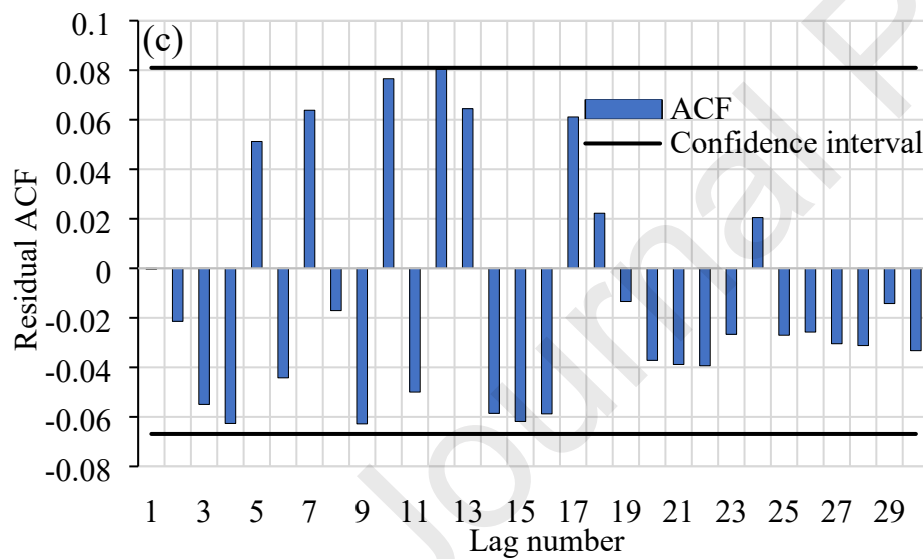
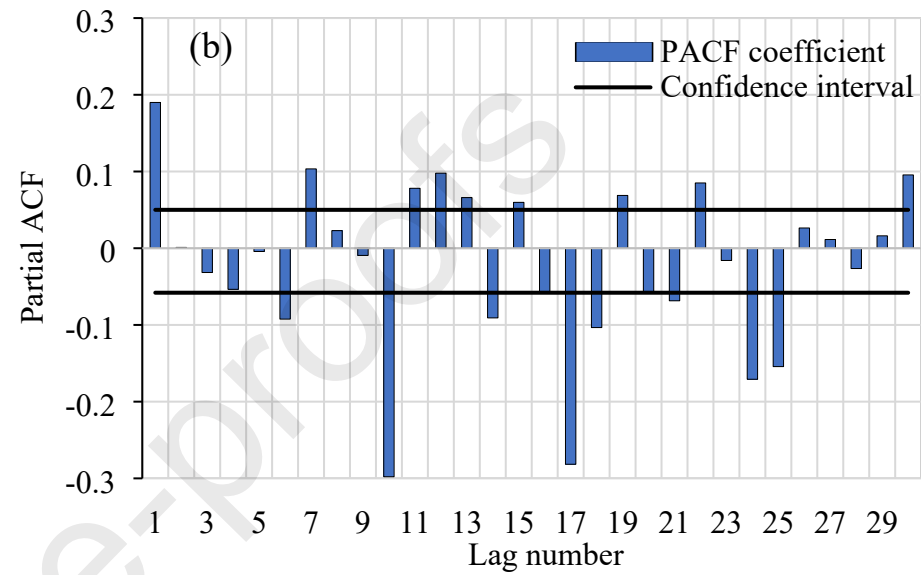
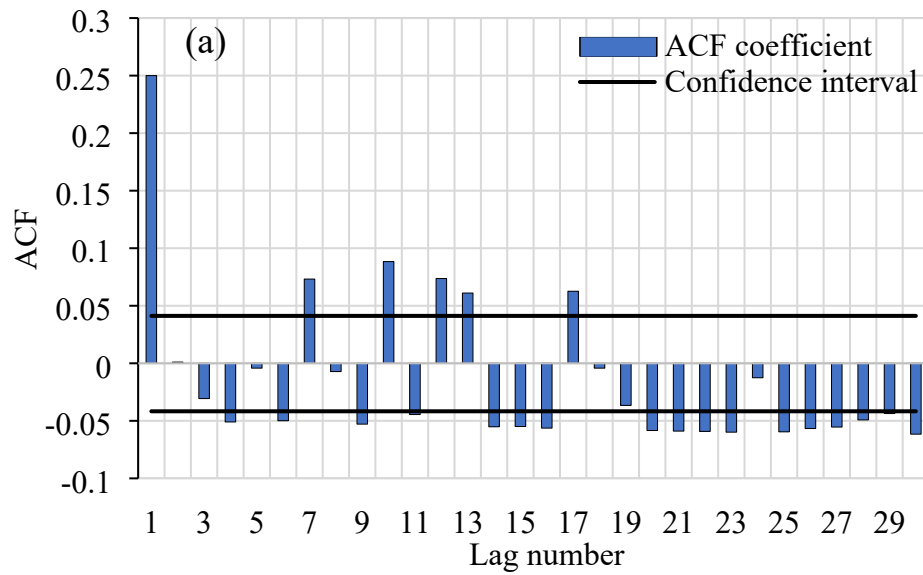
An autoregressive integrated moving average (ARIMA) model is characterised by three parameters, namely autoregressive (p), non-seasonal difference (d), and moving average part (q). As confirmed by the Augmented Dickey–Fuller test, the differencing parameter is set to 0 as no differencing is required because of stationary time series. To determine the other two parameters, autocorrelation function and partial autocorrelation function plots are developed and presented in Figures 8 (a) and (b). In general, the number of lags outside the confidence interval indicates the potential lags to be considered for the autoregressive part (p) and moving average part (q) using partial autocorrelation function and autocorrelation function plots, respectively. As evident from Figures 8 (a) and (b), there are a couple of lags outside the confidence intervals. Therefore, various forms of ARIMA models are developed and compared using three goodness-of-fit measures, including the Bayesian information criterion (BIC), Ljung-Box test (Q^*), and mean absolute error (MAE). These goodness-of-fit measures indicate that the ARIMA (1,0,1) outperforms its competing models (i.e., ARIMA (2,0,1) and ARIMA (3,0,1)) with lower BIC (1127.87) and MAE (5.800E-05) and p -value of Ljung-Box test being greater than 0.05 (Q^* statistic = 17.11; p -value = 0.39).

A similar comparison is also performed for an autoregressive moving average model with exogenous variables (ARIMAX) model, which incorporates the influence of various factors on crash risk. The comparative results suggest that the ARIMAX (1,0,1) outperforms its competing models in terms of goodness-of-fit measures mentioned above.

4.2.4 Model diagnostic

The selected autoregressive integrated moving average models with and without exogenous variables (1,0,1) are further tested to confirm their adequacy for forecasting crash risk at signalised intersections. To this end, autocorrelation function and partial autocorrelation function plots of residuals are developed for each intersection, and a typical illustration for one day of Appleby-Stafford Intersection is shown in Figures 8 (c) and (d). The plots show that residual partial autocorrelation function and autocorrelation function are not significant at any lag (lies within confidence interval), implying that serial correlation is not significant between error terms, suggesting that the selected model is adequate. The overall adequacy of the model is also assessed by Ljung-Box (Q^*) statistics (p -value = 0.39 > assumed $\alpha = 0.05$), which suggests that the model is adequate for forecasting crash risk for future signal cycles. Note that similar findings are obtained for other intersections.

Once the adequacy of the autoregressive integrated moving average models is confirmed, the next step is to apply these models to forecast crash risk for future signal cycles based on the time series of crash risks estimated by the generalised extreme value model. A detailed discussion is presented in the next subsection.



Abbreviations: *ACF*: autocorrelation function; *PACF*: Partial autocorrelation function

Fig. 9. Model diagnostic plots for autoregressive integrated moving average model for Appleby-Stafford intersection

4.2.5 Crash risk forecasting and comparison

The signal cycle level crash risk obtained from the generalised extreme value model is used as the input to the autoregressive integrated moving average model to predict the crash risk for future signal cycles. To this end, two models are developed, namely autoregressive integrated moving average model without exogenous variables (ARIMA) and autoregressive integrated moving average model with exogenous variables (ARIMAX). Several covariates were added to the ARIMAX model to find whether they have a significant relationship with crash risk. One important factor that governs the selection of covariates for an ARIMAX model is that future values of covariate series are needed for every time interval of forecasting. Therefore, the future values of covariates should either be known in advance or should be forecasted. To this end, it has been reported that a multivariate time-series model is only able to give ‘good’ forecasts when the forecasts of explanatory variables can be made (much) more accurately than those of the response variable (Chatfield and Xing, 2021). For this purpose, this study tests only those covariates in the ARIMAX model that are either known for future time intervals or can be obtained with reasonable assumptions. A categorical variable to indicate whether a given time interval (signal cycle) lies within a peak hour or an off-peak hour is added to the ARIMAX model, but this covariate has not been found to be statistically significant. Similarly, traffic flow during a given hour of a typical weekday can be assumed to be the same as the previous day. Therefore, the traffic flow of a signal cycle is used in the ARIMAX model and found to be statistically significant.

Table 4 presents the model estimation results. Separate models are developed for each day for each intersection. It is evident from the results that model goodness-of-fit has improved by adding the traffic flow variable in the autoregressive integrated moving average model. For instance, the Bayesian Information Criterion (BIC) values for four days of the Appleby-Stafford Intersection of the autoregressive integrated moving average model without exogenous variables (ARIMA) are 741.2, 910.6, 525.2, and 710.2, whereas the corresponding BIC values for the autoregressive integrated moving average model with exogenous variables (ARIMAX) are 611.8, 757.2, 486.7, and 579.4.

To further assess the forecasting performance of autoregressive integrated moving average models, mean absolute error and relative absolute error are calculated. The relative absolute error can be computed as the ratio of the mean absolute error to the mean of the observed values (here, crash risks estimated by the extreme value model). Table 4 presents the forecasting results of the two models. Note that crash risk is predicted for each day of each intersection separately, and a typical graphical representation of estimated versus predicted crash risk for one day of all three intersections can be seen in Figure 10.

Table 5 indicates that the autoregressive integrated moving average with exogenous variables (ARIMAX) model predicts the crash risk for future cycles with good accuracy. Note that 70% of the data are used to fit the model, whilst the rest are used for model predictions. The Relative Absolute Errors (RAE) of the ARIMA model (without exogenous variables) for Appleby-Stafford Intersection for four days are 9.88E-01, 2.17E-02, 4.77E-01, and 2.11E-01, respectively, whereas the corresponding errors for the ARIMAX model are 9.10E-01, 2.06E-02, 3.98E-01, and 1.10E-01. These results demonstrate the slightly better forecasting accuracy of the ARIMAX model.

Table 4. Autoregressive integrated moving average models estimation summary.

Intersection n	Covariate	Day 1		Day 2		Day 3		Day 4					
		Estimate (t-stat)		BIC		Estimate (t-stat)		BIC		Estimate (t-stat)		BIC	
		ARIMAX	ARIM A	ARIMA X (ARIMA)	ARIMA X (ARIMA)	ARIM A	ARIMA X (ARIMA)	ARIMA X (ARIMA)	ARIM A	ARIMA X (ARIMA)	ARIM A	ARIMA X (ARIMA)	
Appleby	Intercept	3.30E-04 (3.73)	0.0074 (2.12)		-3.30E-04 (-2.45)	-0.002 (-6.45)		2.11E-04 (3.22)	0.0006 (5.2)		2.05E-04 (5.52)	0.0089 (5.17)	
	Flow	1.30E-04 (2.95)	—	611.8 (741.2)	1.98E-04 (2.55)	—		2.24E-04 (3.92)	—		2.06E-04 (2.56)	—	
	AR1	0.028 (5.83)	0.0024 (4.93)		0.0556 (8.05)	0.1147 (2.24)		0.7201 (2.90)	0.0649 (3.43)		0.7924 (2.38)	0.998 (9.83)	
	MA1	0.1234 (2.74)	0.098 (2.55)		0.2582 (3.72)	0.1231 (6.08)		0.2481 (8.0)	0.2098 (3.56)		0.766 (10.21)	0.0014 (6.3)	

Beaudesert	Intercept	0.0026 (4.33)	0.0016 (4.80)	0.0769 (2.75)	0.0089 (4.25)	1.23E-04 (2.12)	0.0899 (9.93)	1.39E-04 (2.01)	0.0015 (3.63)
	Flow	0.0002 (2.5)	—	0.0046 (11.5)	—	1.22E-04 (2.38)	—	1.55E-04 (3.72)	—
	AR1	0.8702 (10.03)	0.7165 (4.6)	(289.8)	0.7722 (7.11)	0.8878 (5.52)	(258.8) (4.4)	0.495 (1.97)	0.0601 (600.7)
	MA1	0.9999 (20.57)	0.6161 (5.1)	0.9899 (18.71)	0.002 (2.39)	0.6183 (5.14)	0.0964 (4.78)	0.8522 (7.22)	0.6169 (6.07)
Logan	Intercept	0.0091 (2.6)	0.011 (2.7)	1.78E-04 (2.05)	0.0155 (6.5)	0.0356 (10.47)	0.015 (4.72)	0.356 (7.89)	0.0145 (8.2)
	Flow	0.0018 (9.0)	—	124.4 (284.7)	3.01E-04 (2.62)	178.2 (205.1)	0.0074 (2.31)	162.6 (229.6)	0.076 (14.62)
	AR1	0.7138 (28.32)	0.1721 (4.02)	0.5096 (2.37)	0.9989 (14.41)	0.7933 (5.73)	0.9988 (1.98)	0.6214 (6.47)	0.9204 (6.43)

	0.6131	0.0017	0.8898	0.0025	0.8123	0.002	0.6123	0.004
MA1	(13.68)	(12.12)	(5.91)	(3.60)	(7.99)	(2.66)	(5.02)	(10.2)

BIC: Bayesian Information Criterion; ARIMA: Autoregressive integrated moving average model without exogenous variables; ARIMAX: autoregressive integrated moving average model with exogenous variables. “—” indicates that the variable is not included in the model.

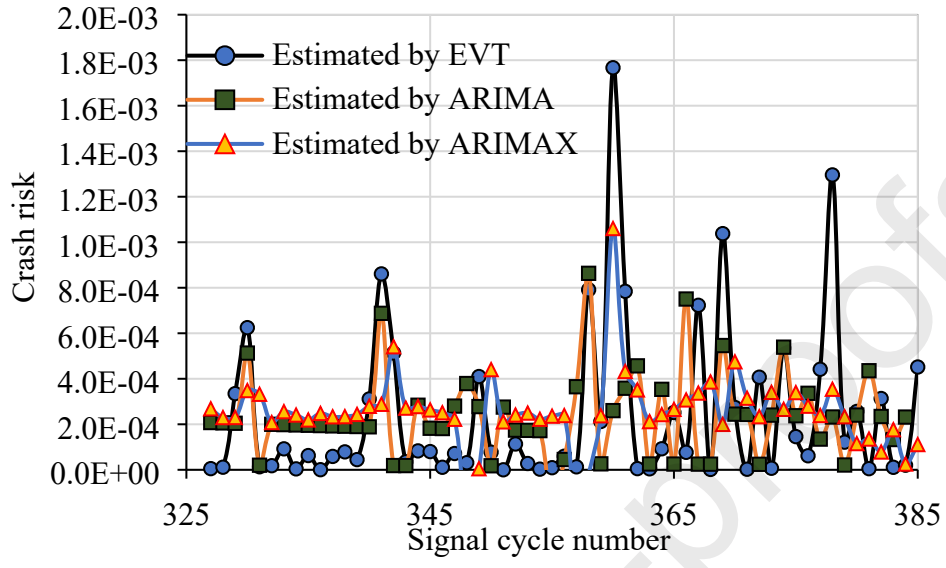
It can be noted from Table 5 that crash risk prediction error varies across sites, whereby the lowest overall error is observed for Appleby-Stafford Intersection (mean RAE of four days = 8.70E-01), and the highest overall error is found for Beaudesert-Granard Intersection (mean RAE of four days = 4.63E+00). An important feature of a real-time safety assessment system is its ability to capture the crash risk variation within different periods of a day, which is described and evaluated in the next subsection. It is also worth investigating for how long in future the crash risk prediction can be made with reasonable accuracy—this question is also answered in the following subsection.

Table 5. Performance of the autoregressive integrated moving average model

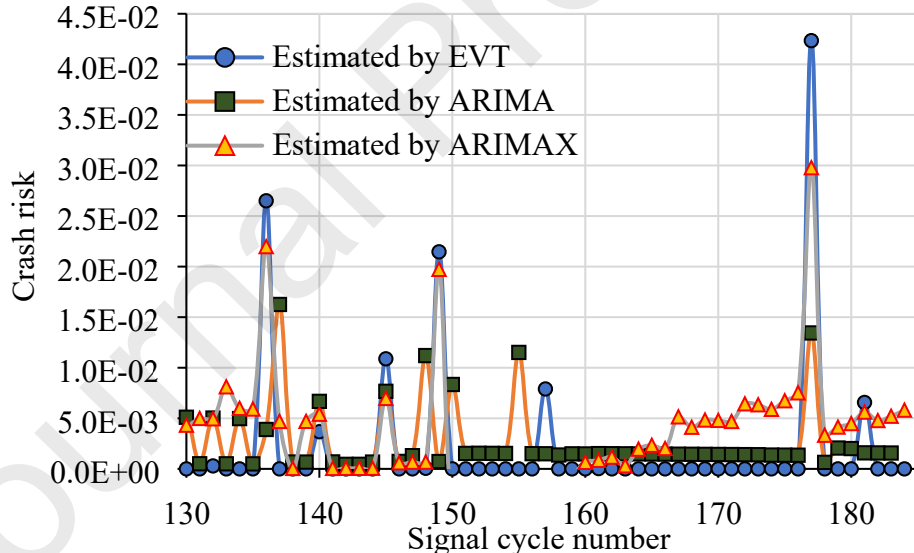
Intersection	Day	ARIMA		ARIMAX	
		MAE	RAE	MAE	RAE
Appleby-Stafford	1	8.20E-04	9.88E-01	2.38E-04	9.10E-01
	2	4.86E-04	2.17E-02	2.69E-04	2.06E-02
	3	3.39E-03	4.77E-01	1.33E-04	3.98E-01
	4	4.38E-03	2.11E-01	1.03E-04	1.10E-01
Beaudesert-Granard	1	5.02E-03	3.01E-03	4.05E-03	1.80E-03
	2	2.07E-02	1.57E-02	1.85E-02	1.54E-02
	3	5.56E-05	9.71E-03	4.80E-05	7.93E-02
	4	5.56E-05	9.71E-01	1.13E-05	7.25E-02
Logan-Kessel	1	1.48E-02	3.10E-02	7.87E-03	1.66E-01
	2	2.06E-02	1.89E-01	7.44E-04	1.70E-01
	3	2.00E-02	2.16E-01	1.53E-02	2.12E-02
	4	1.66E-02	2.19E-02	1.53E-02	2.18E-02

Abbreviations: *BIC*: Bayesian information criterion; *MAE*: Mean absolute error; *RMSE*: root mean square error; *ARIMA*: autoregressive integrated moving average without exogenous variable; *ARIMAX*: autoregressive integrated moving average with exogenous variable.

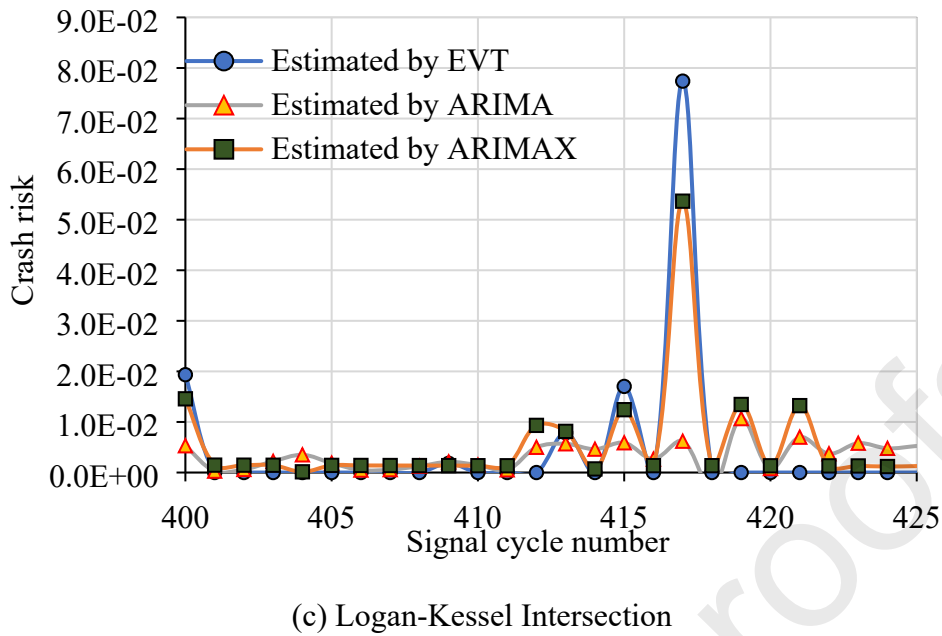
Note that the mean estimated crash risks at the signal cycle level were fed into the ARIMA model for crash risk prediction. To further examine the effects of uncertainties in estimated crash risks for crash predictions, the ARIMA model can be tested for various quantiles (e.g., 75th, 85th, 95th, etc.) of estimated crash risks, which is left for future research.



(a) Appleby-Stafford Intersection



(b) Beaudesert-Granard Intersection



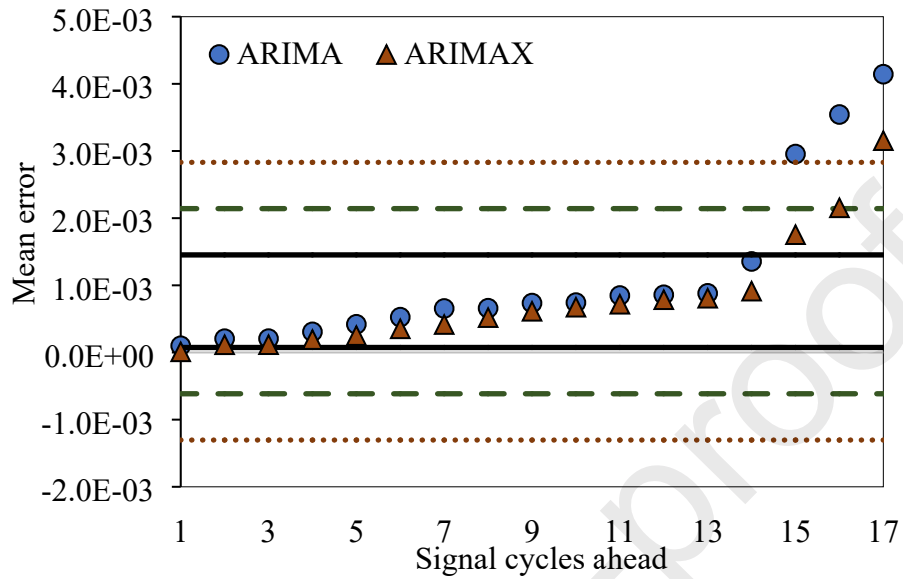
Abbreviations: *EVT: extreme value theory; ARIMA: autoregressive integrated moving average without exogenous variable; ARIMAX: autoregressive integrated moving average with exogenous variable.*

Fig. 10. Crash risk forecasting by the autoregressive moving average models

4.3 Real-time crash risk forecasting outreach

The ability to pre-identify risky traffic conditions is at the heart of a real-time safety analysis framework. Therefore, determining the number of time intervals (here, signal cycles) for which the crash risk can be forecasted with acceptable accuracy is essential. Such knowledge will offer road authorities twofold benefits. First, knowing in advance about the possibility of higher crash risk will lead to devising countermeasures that can minimise the likelihood of a crash. Second, even if a crash is imminent, such knowledge will allow minimising its further impacts on traffic flow. For this purpose, the overall forecasting error (average of mean absolute error of all four days for a given intersection) is calculated. As an example, Figure 11 shows and compares the performance of the autoregressive integrated moving average (ARIMA) model with and without exogenous variables for 17 signal cycles at the Appleby-Stafford Intersection. This figure defines three boundaries based on the standard deviation of prediction error, whereby errors within two standard deviations represent a 95% confidence interval. In general, the errors within one standard deviation imply that the model has relatively smaller errors than three standard deviations. It can be observed that the prediction error of the ARIMA model for 14 signal cycles is within one standard deviation, whilst the prediction of the same model for the 15th signal cycle and onwards is outside three standard deviations. The prediction error for the ARIMAX model is within three standard deviations up to 16 signal cycles, which is two cycles ahead of prediction than that of the ARIMA model. From this figure, it can be concluded that the developed ARIMA and ARIMAX models can reasonably predict future crash risk, with marginally better performance of the latter model. In this case, the ARIMA model predicts crash risk for 14 future cycles, approximately 30-35 minutes ahead, whereas, for the ARIMAX model, the crash risk for 30-38 minutes ahead can be predicted. Another key observation from Figure 11 is that the immediate future signal cycle exhibits lower prediction error, and the error magnifies when the prediction is performed for farther future cycles. Note that although Figure 11 and the aforementioned analysis are for the Appleby-Stafford intersection, similar trends

were observed for the Logan-Kessel intersection and Granard-Beaudesert intersection. Particularly, the crash risk forecasts of ARIMA (and ARIMAX) models for the Logan-Kessel intersection and Granard-Beaudesert intersections are 15 (16) and 12 (14) signal cycles, respectively.



Abbreviation: SD: standard deviation; ARIMA: autoregressive integrated moving average without exogenous variable; ARIMAX: autoregressive integrated moving average with exogenous variable.

Fig. 11. A typical example of forecasting outreach of the autoregressive integrated moving average models for Appleby-Stafford Intersection

4.4 Predicting crash risk variation within a day

For a real-time crash risk forecasting model, it is important to predict the varying crash risk across days and within different periods of a day. A typical day has three notable patterns: morning peak (7 am to 9 am), off-peak (9 am to 4 pm), and evening peak (4 pm to 6 pm). This subsection discusses the results of evaluating the forecasting performance of the autoregressive integrated moving average model with exogenous variables (ARIMAX) for these three periods of the day. Note that this model was selected because it showed better accuracy (refer to the previous section). Table 6 presents the model prediction results for all intersections where the crash prediction error (in terms of relative absolute error) is averaged for each period across four days (e.g., average of morning peak for four days of Appleby-Stafford Intersection). Results reveal that the ARIMAX model shows a reasonable prediction error, with the lowest error observed for off-peak periods. A plausible reason for the relatively lower magnitude of prediction error for an off-peak period could be fewer fluctuations of crash risk. Contrastingly, crash risk fluctuates during peak hours, and the ARIMAX model appears to capture that crash risk, but the prediction error is higher. To this end, more refinements in the current model are suggested to capture such variations.

Table 6. Prediction performance for different periods of day for study intersections

Time periods of a day

Intersection	Morning Peak	Off-Peak	Evening Peak
Appleby-Stafford	5.44E-01	2.17E-02	3.17E-01
Beaudesert-Granard	2.08E-01	4.18E-02	1.43E-01
Logan-Kessel	1.97E-01	3.18E-02	1.99E-01

5. Discussion

The current real-time safety management models lack the ability to analyse the crash risk pattern that forms over time at a road facility and subsequently predict the crash risk on the basis of that spatiotemporal pattern. To bridge this gap, this study presents a modelling framework to forecast the real-time crash risk of signalised intersections. More specifically, a unified framework of extreme value theory and autoregressive integrated moving average time series model has been developed, whereby the former model estimates the crash risks for the short time window, and the latter models this serially correlated data to forecast the crash risks for future periods.

Aligned with the literature (Zheng and Sayed, 2020, Ali et al., 2023b), this study has also adopted the non-stationary generalised extreme value approach to estimate crash risks. One important justification for this selection is to have the ability to incorporate time-varying traffic characteristics so that the dynamic nature of real-time safety analysis can be modelled. Further, along with conventional variables like traffic flow and speed, covariates suitable to characterise the rear-end crash risk in a signal cycle, e.g., shockwave area and platoon ratio, are used to develop the non-stationary model. Among three non-stationary models, the model with covariates included in the location parameter shows the lowest deviance information criterion, suggesting the superior goodness of fit. Some past studies found that introducing covariates in location and scale parameters yields better model fit, which contrasts our findings. A simultaneous parameterisation of location and scale parameters may lead to potential heterogeneity overlap, affecting model performance (Ali et al., 2023b).

The sign convention of the extreme value model parameters is intuitive. For instance, the traffic flow parameter shows a positive relationship with crash risk, indicating that with an increase in traffic flow, rear-end crash risk is likely to increase. The higher number of vehicles within a signal cycle increases the exposure and consequent rear-end crash risk. The relationship can be explained by the fact that more vehicles would like to clear the intersection in a given green signal cycle by following too closely, thereby increasing the chances of rear-end collisions (Zheng and Sayed, 2020). Like the traffic flow parameter, speed is also found to be directly related to crash risk, with higher speeds likely to result in higher rear-end crash risk. Vehicles with higher speeds may apply sudden brakes in response to changes in traffic lights, which may increase their probability of rear-end crash risk (Ali et al., 2021). Similar to these two parameters, the shockwave area is also directly related to crash risk, with a bigger area leading to higher crash risk. A larger shockwave area indicates potentially longer queues being formed at an intersection, which increases the rear-end crash risk because more drivers would

want to clear the intersection area in the next green signal cycle by tailgating their leaders, which deteriorates traffic safety (Michael et al., 2000). The platoon ratio is indirectly associated with rear-end crash risk, suggesting that a higher platoon ratio leads to lower rear-end crash risk. A higher platoon ratio reflects a higher number of vehicles arriving during the green time, which can clear the intersection with a lower chance of rear-end crashes.

To develop the autoregressive integrated moving average model, the signal cycle level crash risk values of the three study intersections have not been combined. In addition, the crash risk values of the signal cycles of one day have been kept separate from those of the other day for the same intersection, as illustrated in Table 4. This step ensures that the assumption of regularly spaced time intervals in a time series is satisfied as the data is only recorded from 6 am to 6 pm for each day. Consequently, the crash risk time series (as illustrated in Figure 7) does not exhibit any trend or seasonal pattern, mainly due to this short data collection period. Therefore, the effect of temporal and seasonal indicators on the crash risk could not be analysed. In this context, a worthwhile research direction would be applying the proposed modelling framework to a larger dataset with continuous collection periods.

The study results demonstrate that, on average, the best model, i.e., autoregressive integrated moving average model with exogenous variables, can forecast the crash risk for 15 signal cycles with reasonable accuracy, which translates to about 30 to 38 minutes ahead. This advance prediction is a key benefit for developing a proactive safety management system, as obtaining the crash risk insights in advance would enable the timely and effective implementation of countermeasures. Notably, the ability to forecast the crash risk based on its spatiotemporal trend also addresses the challenge of keeping the latency to a minimum, where latency refers to the time it takes to process the data and extract real-time safety insights from it.

6. Conclusions and Future Recommendations

This study developed a unified real-time crash risk forecasting framework for signalised intersections. A Bayesian non-stationary Block Maxima model, corresponding to generalised extreme value distribution, was developed and applied to rear-end conflicts in a signal cycle identified by a modified time-to-collision measure. Using the automated covariate extraction algorithm, signal cycle level covariates were extracted and used as input to the Bayesian generalised extreme value model to capture heterogeneity associated with time-varying crash risk. Crash risk corresponding to each signal cycle was obtained, forming time series data. To forecast the crash risk for future cycles based on the historical trend of crash risks of past/present signal cycles, the autoregressive integrated moving average model was developed.

The developed generalised extreme value model was estimated using the video data recorded at three signalised intersections in Queensland, Australia. An automated video data processing platform was used to convert the videos into trajectories and obtain traffic conflicts at the signal cycle level. Covariates to characterise the rear-end crash risk were incorporated in the model, which was generally found to outperform the stationary model in terms of accurate mean crash estimates and narrower confidence intervals. In particular, the model with parameterised location parameter performed the best.

The best-performing generalised extreme value model was used to estimate signal cycle-level crash risk, which served as the baseline for developing the autoregressive integrated moving average (ARIMA) model. The forecasting outreach of the ARIMA model suggests that the model can reasonably predict the crash risk up to 25~35 minutes in advance. Finally, the

ARIMA model was applied to predict the crash risk variation within different periods of a day and was found to predict crash risk with good accuracy. The proposed framework helps identify the spatiotemporal windows where safety gradually deteriorates over time, thus enabling proactive safety assessment.

Due to the unavailability of actual crash risk data at the signal cycle level, this study considered crash risk estimated from the generalised extreme value model as an input to the autoregressive integrated moving average (ARIMA) model. Recognising the uncertainty associated with the generalised extreme value model estimates that can further exacerbate in the ARIMA model, it becomes paramount to test the model on data without uncertainties or where the ground truth is known. To this end, synthetic crash risk profiles could be meticulously generated and rigorously tested to evaluate the true performance of the ARIMA model. Another limitation of this study is the short data collection period (4 days), due to which the effect of temporal or seasonal indicators could not be analysed in the ARIMA model. Future studies with larger data collection periods should investigate this important aspect. Further, since this study developed the autoregressive integrated moving average (ARIMA) model either without covariates or with covariates, an interesting research direction could be using the observed conflicts and covariates to forecast future conflicts and covariates, which can be then used to estimate future crash risks. In doing so, a comparison can be made between the method adopted in this study and the proposed method. It is worth noting that this study followed existing studies (Arun et al., 2021a, Zheng and Sayed, 2020) for automated conflict extraction, which uses time-to-collision with a threshold of 3 s. However, as recent studies have demonstrated the suitability of modified time-to-collision measure instead of time-to-collision to model rear-end conflicts in extreme value models, there is a need to update automated conflict extraction with an adequate threshold of modified time-to-collision, for which concrete evidence is yet to be established. Meanwhile, although the developed model is validated at the aggregated level, one concern remains whether the model will be able to replicate the same performance when validated at the disaggregated level. To this end, the estimated conflict frequency (less than a certain threshold) for a given signal cycle can be compared to the observed conflict frequency in the same signal cycle, allowing a comparison of conflicts at signal cycle level. Finally, this study applied the block maxima approach for crash risk estimation, whereas investigating crash risk forecasting based on a peak over threshold model merits an investigation, which is ongoing.

Acknowledgment

This research is partially funded by the Queensland University of Technology, iMOVE CRC, and supported by the Cooperative Research Centres program, an Australian Government initiative. The authors would also like to acknowledge Transport and Mains Roads (TMR), Queensland, for providing video data.

References

- Ali, Y., Haque, M. and Mannering, F. 2023a. Assessing traffic conflict/crash relationships with extreme value theory: Recent developments and future directions for connected and

autonomous vehicle and highway safety research. *Analytic Methods in Accident Research*, 100276.

Ali, Y., Haque, M. and Mannering, F. 2023b. A Bayesian generalised extreme value model to estimate real-time pedestrian crash risks at signalised intersections using artificial intelligence-based video analytics. *Analytic Methods in Accident Research*, 38, 100264.

Ali, Y., Haque, M. and Zheng, Z. 2022a. Assessing a Connected Environment's Safety Impact During Mandatory Lane-Changing: A Block Maxima Approach. *IEEE Transactions on Intelligent Transportation Systems*.

Ali, Y., Haque, M. and Zheng, Z. 2022b. An Extreme Value Theory approach to estimate crash risk during mandatory lane-changing in a connected environment. *Analytic Methods in Accident Research*, 33, 100193.

Ali, Y., Haque, M., Zheng, Z. and Bliemer, M. 2021. Stop or go decisions at the onset of yellow light in a connected environment: A hybrid approach of decision tree and panel mixed logit model. *Analytic Methods in Accident Research*, 31, 100165.

AMAG. 2021. *Smart SafetyTM, Brisbane, Australia*

Arun, A., Haque, M., Bhaskar, A., Washington, S. and Sayed, T. 2021a. A bivariate extreme value model for estimating crash frequency by severity using traffic conflicts. *Analytic Methods in Accident Research*, 32, 100180.

Arun, A., Haque, M., Bhaskar, A., Washington, S. and Sayed, T. 2021b. A systematic mapping review of surrogate safety assessment using traffic conflict techniques. *Accident Analysis and Prevention*, 153, 106016.

Arun, A., Haque, M., Washington, S., Sayed, T. and Mannering, F. 2021c. A systematic review of traffic conflict-based safety measures with a focus on application context. *Analytic Methods in Accident Research*, 32, 100185.

Bao, J., Liu, P. and Ukkusuri, S. 2019. A spatiotemporal deep learning approach for citywide short-term crash risk prediction with multi-source data. *Accident Analysis and Prevention*, 122, 239-254.

Basso, F., Pezoa, R., Varas, M. and Villalobos, M. 2021. A deep learning approach for real-time crash prediction using vehicle-by-vehicle data. *Accident Analysis and Prevention*, 162, 106409.

Box, G. and Jenkins, G. 1976. *Time series analysis: forecasting and control*, Holden-Day, San Francisco.

Cai, B. and Di, Q. 2023. Different Forecasting Model Comparison for Near Future Crash Prediction. *Applied Sciences*, 13 (2), 759.

Castanedo, F. 2013. A review of data fusion techniques. *The Scientific World Journal*.

Chen, F., Chen, S. and Ma, X. 2018. Analysis of hourly crash likelihood using unbalanced panel data mixed logit model and real-time driving environmental big data. *Journal of Safety Research*, 65, 153-159.

- Chung, K., Jang, K., Madanat, S. and Washington, S. 2011. Proactive detection of high collision concentration locations on highways. *Procedia-social and Behavioral Sciences*, 17, 634-645.
- Dickey, D. and Fuller, W. 1979. Distribution of the estimators for autoregressive time series with a unit root. *Journal of the American Statistical Association*, 74 (366a), 427-431.
- Ding, H., Lu, Y., Sze, N., Chen, T., Guo, Y. and Lin, Q. 2022. A deep generative approach for crash frequency model with heterogeneous imbalanced data. *Analytic Methods in Accident Research*, 34, 100212.
- Farah, H. and Azevedo, C. 2017. Safety analysis of passing maneuvers using extreme value theory. *IATSS Research*, 41 (1), 12-21.
- Fu, C. and Sayed, T. 2022a. Bayesian dynamic extreme value modeling for conflict-based real-time safety analysis. *Analytic Methods in Accident Research*, 34, 100204.
- Fu, C. and Sayed, T. 2022b. A multivariate method for evaluating safety from conflict extremes in real time. *Analytic Methods in Accident Research*, 36, 100244.
- Hassouna, F. and Pringle, I. 2019. Analysis and prediction of crash fatalities in Australia. *The Open Transportation Journal*, 13, 134-140.
- HCM 2000. Highway capacity manual. *Washington, DC*.
- Hussain, F., Li, Y., Arun, A. and Haque, M. 2022. A hybrid modelling framework of machine learning and extreme value theory for crash risk estimation using traffic conflicts. *Analytic Methods in Accident Research*, 36, 100248.
- Lee, C., Hellinga, B. and Saccomanno, F. 2003. Real-time crash prediction model for application to crash prevention in freeway traffic. *Transportation Research Record*, 1840 (1), 67-77.
- Li, P., Abdel-Aty, M. and Yuan, J. 2020. Real-time crash risk prediction on arterials based on LSTM-CNN. *Accident Analysis and Prevention*, 135, 105371.
- Ljung, G. and Box, G. 1978. On a measure of lack of fit in time series models. *Biometrika*, 65 (2), 297-303.
- Machiani, S. and Abbas, M. 2016. Safety surrogate histograms (SSH): A novel real-time safety assessment of dilemma zone related conflicts at signalized intersections. *Accident Analysis and Prevention*, 96, 361-370.
- May, A. 1990. Traffic flow fundamentals prentice hall. *Inc. Egglewood Cliffs, NJ, USA*.
- Michael, P., Leeming, F. and Dwyer, W. 2000. Headway on urban streets: observational data and an intervention to decrease tailgating. *Transportation Research Part F*, 3 (2), 55-64.
- Mussone, L., Bassani, M. and Masci, P. 2017. Analysis of factors affecting the severity of crashes in urban road intersections. *Accident Analysis and Prevention*, 103, 112-122.

- Noland, R., Quddus, M. and Ochieng, W. The effect of the congestion charge on traffic casualties in London: an intervention analysis. *Transportation Research Board (TRB) Annual Meeting*, Washington, DC, USA, January, 2006.
- Ozbay, K., Yang, H., Bartin, B. and Mudigonda, S. 2008. Derivation and validation of new simulation-based surrogate safety measure. *Transportation research record*, 2083 (1), 105-113.
- Quddus, M. 2008. Time series count data models: an empirical application to traffic accidents. *Accident Analysis and Prevention*, 40 (5), 1732-1741.
- Roshandel, S., Zheng, Z. and Washington, S. 2015. Impact of real-time traffic characteristics on freeway crash occurrence: Systematic review and meta-analysis. *Accident Analysis and Prevention*, 79, 198-211.
- Songchitruksa, P. and Tarko, A. 2006. The extreme value theory approach to safety estimation. *Accident Analysis and Prevention*, 38 (4), 811-822.
- Spiegelhalter, D., Best, N., Carlin, B. and Van Der Linde, A. 2002. Bayesian measures of model complexity and fit. *Journal of the Royal Statistical Society*, 64 (4), 583-639.
- Tarko, A. 2012. Use of crash surrogates and exceedance statistics to estimate road safety. *Accident Analysis and Prevention*, 45, 230-240.
- Wang, L., Abdel-Aty, M., Lee, J. and Shi, Q. 2019. Analysis of real-time crash risk for expressway ramps using traffic, geometric, trip generation, and socio-demographic predictors. *Accident Analysis and Prevention*, 122, 378-384.
- Xu, C., Tarko, A., Wang, W. and Liu, P. 2013. Predicting crash likelihood and severity on freeways with real-time loop detector data. *Accident Analysis and Prevention*, 57, 30-39.
- Yasmin, S., Eluru, N., Wang, L. and Abdel-Aty, M. 2018. A joint framework for static and real-time crash risk analysis. *Analytic Methods in Accident Research*, 18, 45-56.
- Yu, R. and Abdel-Aty, M. 2013. Utilizing support vector machine in real-time crash risk evaluation. *Accident Analysis and Prevention*, 51, 252-259.
- Yuan, J. and Abdel-Aty, M. 2018. Approach-level real-time crash risk analysis for signalized intersections. *Accident Analysis and Prevention*, 119, 274-289.
- Yuan, J., Abdel-Aty, M., Gong, Y. and Cai, Q. 2019. Real-time crash risk prediction using long short-term memory recurrent neural network. *Transportation Research Record*, 2673 (4), 314-326.
- Zhang, S. and Abdel-Aty, M. 2022. Real-time crash potential prediction on freeways using connected vehicle data. *Analytic Methods in Accident Research*, 36, 100239.
- Zheng, L., Ismail, K. and Meng, X. 2014. Freeway safety estimation using extreme value theory approaches: A comparative study. *Accident Analysis and Prevention*, 62, 32-41.

- Zheng, L. and Sayed, T. 2019. Bayesian hierarchical modeling of traffic conflict extremes for crash estimation: a non-stationary peak over threshold approach. *Analytic methods in accident research*, 24, 100106.
- Zheng, L. and Sayed, T. 2020. A novel approach for real time crash prediction at signalized intersections. *Transportation Research Part C*, 117, 102683.
- Zheng, L., Sayed, T. and Essa, M. 2019. Bayesian hierarchical modeling of the non-stationary traffic conflict extremes for crash estimation. *Analytic methods in accident research*, 23, 100100.
- Zheng, L., Sayed, T. and Mannering, F. 2021. Modeling traffic conflicts for use in road safety analysis: A review of analytic methods and future directions. *Analytic Methods in Accident Research*, 29, 100142.

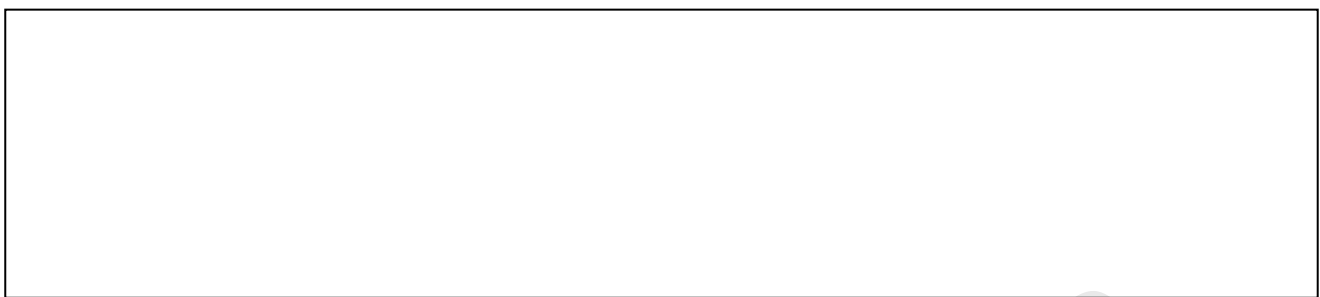
Highlights

- A framework of extreme value theory and autoregressive integrated moving average method is developed
- A Bayesian generalised extreme value model estimates the crash risk at signal cycle levels
- An autoregressive integrated moving average model is applied to time series of crash risk
- The framework can reasonably estimate future crash risk at signalised intersections

Declaration of interests

The authors declare that they have no known competing financial interests or personal relationships that could have appeared to influence the work reported in this paper.

The authors declare the following financial interests/personal relationships which may be considered as potential competing interests:



Journal Pre-proofs